NATIONAL ADVISORY COMMITTEE FOR AERONAUTICS

WARTIME REPORT

ORIGINALLY ISSUED

April 1945 as
Memorandum Report L5C29

TWO-DIMENSIONAL WIND-TUNNEL INVESTIGATION OF SPOILER

AILERON FLAP MODEL FOR THE HUGHES XF-11 AIRPLANE

By William J. Underwood and Felicien F. Fullmer, Jr.

Langley Memorial Aeronautical Laboratory
Langley Field, Va.

NACA

WASHINGTON
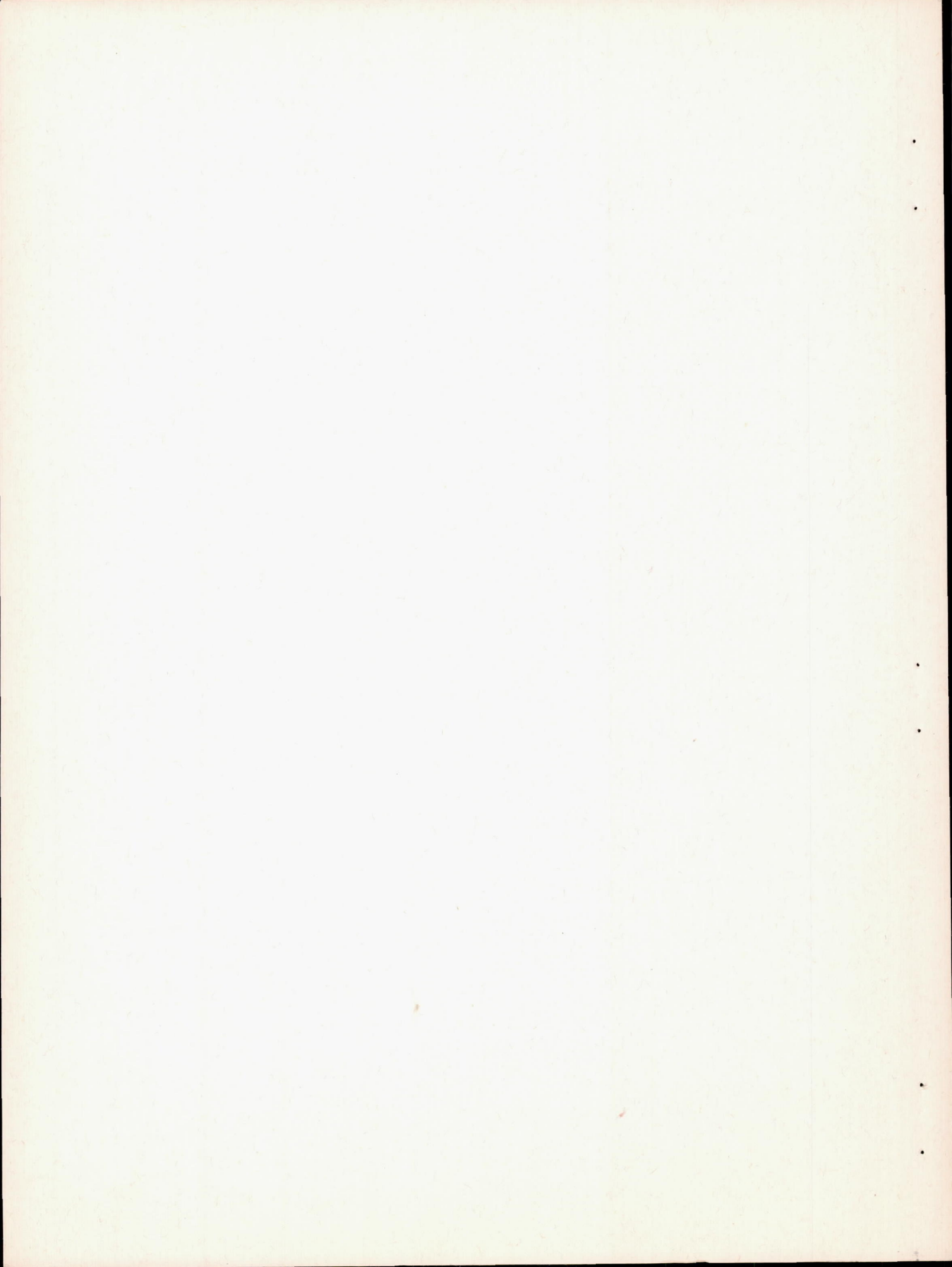
NATIONAL ADVISORY COMMITTEE FOR AERONAUTICS

MEMORANDUM REPORT

for the

Army Air Forces, Air Technical Service Command

TWO-DIMENSIONAL WIND TUNNEL INVESTIGATION OF SPOILER

AILERON FLAP MODEL FOR THE HUGHES XF-11 AIRPLANE

By William J. Underwood and Felicien F. Fullmer, Jr.

SUMMARY

An investigation was made in the Langley two-dimensional low-turbulence tunnels of a retractable spoiler aileron on the NACA 66(215)-216 (approx.) airfoil with a 25-percent-chord slotted flap. The spoiler aileron, essentially a curved thin plate arranged to rotate about a hinge at the center of curvature, moved edgewise into and out of the wing through a narrow slot in the upper surface at 75 percent of the airfoil chord. The effect of spoiler thickness, spoiler gap, spoiler bevel angle, spoiler roughness, and flap deflection on the aerodynamic characteristics of the spoiler aileron are presented herein.

The results indicate that the hinge-moment characteristics of the retractable spoiler aileron were greatly affected by spoiler thickness, rear-gap size, and the bevel angle of the upper face of the spoiler. The best hinge-moment characteristics of the configurations tested were obtained with the thinnest (0.0028c) spoiler which had a 17° bevel angle on the upper and lower faces and roughness on the upper face, the largest (0.0100c) spoiler rear gap, and the 0.0013c spoiler forward gap. The spoiler aileron was effective in producing a substantial decrease in the section lift coefficient for all negative spoiler deflections larger than -3°. The spoiler effectiveness parameter $\Delta\alpha_0/\Delta\delta_s$ for deflections above -10° was practically unaffected by increasing the test Reynolds number from 2.5 to 6 million. With the spoiler in the retracted position, air flow through the cut-outs for the spoiler in the upper surface of the airfoil caused an increase of approximately 12 percent in the minimum profile-drag coefficient. The increments

of section pitching-moment coefficient of the airfoil
produced by the spoiler aileron were less positive than
those produced by a plain sealed flap of equal effec-
tiveness. The advantage of the smaller increments of
section pitching moment associated with spoiler ailerons
with respect to the lateral-control reversal speed of an
airplane, however, may be offset by the relatively larger
span required for spoiler ailerons.

INTRODUCTION

At the request of the Army Air Forces, Air Technical
Service Command, tests were conducted to determine the
section aerodynamic characteristics of the NACA 66(215)-216
(approx.) airfoil section equipped with a slotted flap
and a retractable spoiler aileron. This investigation
was carried out for the purpose of furnishing section
aerodynamic data for a retractable spoiler aileron to
be used in combination with 20-percent-chord internally
balanced ailerons for lateral control with approximately
a 90-percent-semispan slotted flap for the wing of the
Hughes XF-11 airplane (fig. 1). The internally balanced
aileron, located outboard of the slotted flap, was
designed to be used as a feeler aileron which requires
that the wheel force due to deflection of the spoiler
aileron be small in magnitude as compared to the wheel
force resulting from deflection of the feeler aileron.

Tests to determine the spoiler load, effectiveness,
hinge-moment, and airfoil profile-drag characteristics
were carried out in the Langley two-dimensional low-
turbulence tunnel. Additional tests at a higher Reynolds
number to determine the spoiler effectiveness, airfoil
profile drag, and pitching moment were carried out in
the Langley two-dimensional low-turbulence pressure
tunnel.

SYMBOLS AND COEFFICIENTS

α_o airfoil section angle of attack

c_l airfoil section lift coefficient

c_{d_o} airfoil section profile-drag coefficient

$c_{m_c/4}$ airfoil section pitching-moment coefficient about quarter-chord point

q_o free-stream dynamic pressure

δ_s spoiler aileron deflection, positive when the upper face is deflected below airfoil upper surface

δ_f flap deflection, positive when the trailing edge is deflected down

H_o free-stream total pressure

p local static pressure

S pressure coefficient $\left(\dfrac{H_o - p}{q_o}\right)$

h spoiler aileron hinge moment, positive when spoiler tends to retract into recess

R_m mean radius of spoiler aileron

t thickness of spoiler aileron

b_s span of spoiler aileron

c_h spoiler aileron section hinge-moment coefficient $\left(\dfrac{h}{q_o R_m t b_s}\right)$

Δc_l increment in section lift coefficient due to spoiler aileron deflection measured at a constant angle of attack

$\Delta\alpha_o$ increment of section angle of attack due to spoiler aileron deflection measured at a constant lift coefficient

$\dfrac{\Delta\alpha_o}{\Delta\delta_s}$ section aileron effectiveness parameter, ratio of change in section angle of attack to increment of spoiler aileron deflection to maintain constant lift

$\Delta c_{m_c/4}$ increment of section pitching-moment coefficient at constant lift due to spoiler aileron deflection

MODEL

A cast aluminum model having a 24-inch chord and 35.62-inch span was made to correspond to the contour of an intermediate section of the wing of the Hughes XF-11 airplane (fig. 2). The model was equipped with a 25-percent-chord slotted flap. The ordinates of the airfoil including the flap are given in table I.

A retractable spoiler aileron having a span of 33.44 inches was installed at the 75-percent-chord station and rotated about a hinge axis at a point 66.4 percent chord aft of the leading edge and 5.31 percent chord above the chord line of the airfoil. Inasmuch as the width of the tunnel-test section is 36 inches, a gap of approximately 1.25 inches existed between each end of the spoiler and the tunnel wall. The spoiler aileron retracted through the upper surface into a recess within the airfoil contour. The model was so designed that the thickness of the spoiler aileron and the rear gap between the spoiler rear face and the upper surface of the airfoil could be varied. The forward gap between the spoiler front face and the upper surface was held constant at 0.13 percent chord regardless of the spoiler thickness or rear-gap size. A sketch of the general model arrangement showing the spoiler and spoiler-slot details is given in figure 3. As shown in figure 3, the spoiler aileron was a curved plate with the original upper and lower faces formed by radial lines through the hinge axis. During the investigation the upper and lower faces of the spoiler were beveled as shown in figure 3. Hereafter the angle between the original radial and the altered surface will be referred to as the bevel angle. With a bevel angle of 17°, both the upper and lower faces of the spoiler were parallel to the airfoil surface when they emerged from the air-foil. The spoiler aileron was supported along the span of the model by webs (figs. 2(a) and 3) located at 5.03 inches and 14.97 inches either side of the center line of the model span. To allow free movement of these webs for full spoiler deflection, chordwise slots were cut at the four positions as previously noted. A typical cut-out in the upper surface is shown in figure 4. Pressure orifices were installed in the center of the span of the 1.04-percent-chord-thick spoiler at positions shown in figure 5 and in the aileron recess at the positions shown in figure 3.

The relation between spoiler deflection in degrees as presented in the results herein to spoiler projection in percent chord is shown in figure 6.

APPARATUS AND TESTS

Lift, drag, and pitching-moment measurements of the model were made by the methods described in reference 1. The hinge moment of the spoiler aileron was measured by means of a calibrated torque rod. The following factors were applied to correct the tunnel data to free-air conditions:

$$c_l = 0.977c_l'$$

$$c_{d_o} = 0.989c_{d_o}'$$

$$c_{m_{c/4}} = 0.989c_{m_{c/4}}'$$

$$\alpha_o = 1.015\alpha_o'$$

where the primed quantities represent the values measured in the tunnel.

Table II gives the model configurations tested in the Langley two-dimensional low-turbulence tunnel at a dynamic pressure of approximately 53 pounds per square foot, which corresponds to a Reynolds number of 2.5 million and a Mach number of 0.18. Configuration 9 of table II was also tested in the Langley two-dimensional low-turbulence pressure tunnel at a dynamic pressure of approximately 76 pounds per square foot and a tank pressure of 60 pounds per square inch, which corresponds to a Reynolds number of 6.0 million and a Mach number of 0.11.

The roughness applied to the upper face of the spoiler aileron for configurations 7 and 9 consisted of 0.01-inch carborundum crystals imbedded in shellac.

RESULTS AND DISCUSSION

The results of this investigation are presented in table III and figures 7 to 20. The surface pressures

obtained over the spoiler surface and in the spoiler
recess are presented in table III in the form of the
pressure coefficient S and should provide data for the
structural design of the spoiler.

Hinge-moment characteristics of spoiler aileron.-
The effect of a decrease in spoiler aileron rear gap
on the hinge-moment coefficients of the 1.04-percent-
chord-thick spoiler is shown in figure 7. A study of
figure 7(a) shows that the hinge-moment coefficients of
the spoiler aileron at an angle of attack of 0° vary
irregularly with spoiler deflection and excessively
high positive hinge-moment coefficient exists at spoiler
deflections of approximately -2° and -50°. As the rear-
gap size was decreased, the hinge-moment coefficients
became more negative and the irregular variation of the
hinge-moment coefficients increased to such an extent
that finally the spoiler (configuration 4) became over-
balanced through the greater part of the deflection
range. The effect of reducing the rear gap was approxi-
mately the same for an angle of attack of 7.11° as for
an angle of attack of 0°. Increasing the angle of
attack also caused the high positive hinge-moment
coefficients for small negative spoiler deflections to
be reduced. The hinge-moment characteristics of the
spoiler aileron were approximately the same for the
flap retracted and deflected conditions (fig. 7(b)).
Since the hinge moment of the spoiler aileron is due
to the difference in the pressures on the upper and
lower faces of the spoiler, a rapid change in these
pressures will cause a corresponding change in the
hinge moment. This pressure change accounts for the
rapid change in the hinge-moment coefficient just as
the upper face of the spoiler emerges from the recess.

If the following airplane dimensions and conditions
are assumed:

Wing area, square feet 989
Weight, pounds 48,000
Control wheel diameter, feet 1.25
Area moment of (one) spoiler aileron upper
   face about the hinge axis, cubic foot   0.28
Mechanical advantage $\begin{cases} (3^{\circ} < \delta_s < -3^{\circ}) \dots \dots \quad 4 \\ (-45^{\circ} < \delta_s < -51^{\circ}) \dots \dots \quad 1 \end{cases}$

the approximate wheel force at 400 miles per hour at 15,000 feet required to hold the spoiler aileron configuration 1 (fig. 7(a)) at a deflection of -2° would be 7.6 pounds and at -50°, 42 pounds. From the hinge-moment characteristics (fig. 7) and from the approximate wheel-force calculations it was apparent that the wheel force due to deflection of the 0.0104c-thick spoiler with any of the rear-gap sizes tested would be uneven and, at times, excessive. In order to reduce the absolute magnitude of the spoiler hinge moments, the thickness of the spoiler was reduced from 0.0104c to 0.0028c. Attempts were made to reduce the irregular variation of hinge-moment coefficient with spoiler deflection by beveling the faces of the spoiler.

The effect of various bevel angles of the upper and lower faces of the thin spoiler is shown in figure 8. A comparison of the hinge-moment characteristics of configuration 1 (fig. 7) with configurations 5 and 8 (fig. 8) shows that, in general, beveling the upper and lower faces and reducing the thickness of the spoiler caused the peak hinge-moment coefficients occurring at spoiler deflections of -2° and -50° to be opposite in sign and approximately half the magnitude of the curve for configuration 1. Comparison of the data for various bevel angles at low angles of attack presented in figure 8 shows that the hinge-moment characteristics for small deflections are extremely sensitive to relatively small changes in the bevel angle. As the spoiler lower face emerges from the recess at a deflection of -47° (fig. 6), the hinge-moment coefficients showed a rapid change at negative deflections greater than approximately -45° as a result of air flow under the spoiler lower face.

The effect on the hinge-moment characteristics of applying roughness to the upper face of the spoiler is shown by comparing figures 8 and 9. It can be seen that the application of roughness to the upper face of the spoiler (configuration 9) eliminated some of the irregularities in the hinge-moment-coefficient curves near 0° spoiler deflection. This change is believed to be due to the roughness causing irregular flow of the air over the upper face of the spoiler aileron as it emerged from the recess and this irregular flow, in turn, tended to spread the rapid changes in pressure loading which were responsible for the unstable hinge-moment characteristics near zero spoiler deflection over a larger range of spoiler deflections. These results would indicate that further improvement in the hinge-moment characteristics could be obtained by scalloping

the upper face of the spoiler spanwise or by rigging the
spoiler in such a manner that the various sections of
the spoiler along the wing span would not emerge from
the recess at the same time.

The hinge-moment coefficients for spoiler aileron
configuration 9 are presented in figure 10 for various
angles of attack at flap deflections of $0°$, $20°$, and $40°$.
With increasing angle of attack the large change in
hinge-moment coefficients for small deflections was
reduced with the result that the hinge-moment coefficients
varied almost linearly with spoiler deflection at the
higher angles of attack. If the aforementioned airplane
dimensions and conditions are again assumed, the approxi-
mate wheel force at 400 miles per hour at 15,000 feet
required to hold the spoiler aileron configuration 9 at
a deflection of $-2°$ would be 3.3 pounds and at $-45°$,
12 pounds. From the hinge-moment characteristics (fig. 10)
and from the approximate wheel-force calculations it was
apparent that the wheel forces corresponding to the
observed hinge-moment coefficients of spoiler aileron
configuration 9 between deflections of $3°$ and $-45°$ would
be small in magnitude as compared to the wheel forces
due to the deflection of the feeler ailerons. Furthermore,
to obtain a smooth variation in the wheel force for
small deflections of the control wheel, it would seem
advantageous to rig the spoiler and feeler ailerons in
such a manner that the negative deflection of the spoiler
would lag the deflection of the upgoing feeler aileron
by several degrees.

Effectiveness of spoiler aileron.- The effect of
changes in the spoiler rear-gap size, bevel angle, and
the application of roughness to the upper face of the
spoiler on the section lift characteristics was small,
as shown in figures 7, 8, and 9. As mentioned previously,
at a deflection of $-47°$ the lower face of the spoiler
emerges from the recess and the thin spoiler aileron at
that deflection becomes ineffective in producing any
further change in the section lift coefficient.

The effect of angle of attack and flap deflection
on the section lift characteristics of the airfoil
produced by the deflection of the spoiler aileron is
presented in figures 10 and 11. Inasmuch as the spoiler
aileron, since it is used on only one wing at a time,
does not operate at approximately constant lift as with
conventional ailerons but at some condition between

constant lift and constant angle of attack, an analysis
of the effectiveness of the spoiler aileron has been made
at both constant angle of attack and constant lift.

The effect of changes in the angle of attack and
flap deflection on the increment of section lift coef-
ficient Δc_l due to spoiler deflection is shown in
figures 12 and 13. In general, the increment Δc_l due
to a given deflection of the spoiler decreased as the
angle of attack was increased (fig. 12). Between angles
of attack of approximately 0° to 7° at $\delta_f = 0^\circ$,
-4° to 4° at $\delta_f = 20^\circ$, 2° to 9° at $\delta_f = 40^\circ$, increasing
the test Reynolds number from 2.5 to 6 million caused
a decrease in the increment Δc_l or effectiveness of
the spoiler aileron when based on the constant angle-
of-attack conception. At the higher angles of attack,
the increment Δc_l increased with Reynolds number.
This effect was caused by an increase in the lift and
lift-curve slope at the higher angles of attack with
the spoiler neutral, similar to that shown in figure 14,
in combination with a decrease in the lift-curve slope
with the spoiler deflected up. The increment Δc_l for
all spoiler deflections increased with flap deflection
up to 20° (fig. 13). At a flap deflection of 40° the
increment Δc_l increased further for spoiler deflections
greater than -10° and decreased for spoiler deflections
less than and including -10°. The results at a flap
deflection of 40° (fig. 12) show that for a Reynolds
number of 6 million a spoiler deflection of -3° was
ineffective in producing any change in the lift at
angles of attack less than 7°.

The effectiveness of the spoiler aileron based on
the constant lift conception is shown in figure 15.
It can be seen that the effectiveness parameter $\Delta\alpha_0/\Delta\delta_s$
varied considerably with spoiler deflection and only
slightly with lift coefficient except for spoiler
deflections of -3° and -10°. Increasing the flap
deflection from 0° to 40° caused the effectiveness
parameter to increase for spoiler deflections larger
than -10°. Increasing the test Reynolds number from
2.5 to 6 million caused only a slight change in the
effectiveness parameter for spoiler deflections larger
than -10°. Within the Reynolds number range investigated,
therefore, it is apparent that only if the spoiler effec-
tiveness analysis is based on the constant angle-of-attack
conception instead of constant lift will scale effect
cause an appreciable decrease in the spoiler effectiveness.

The increment $\Delta\alpha_o$ due to deflecting the spoiler aileron to -45° would be 7.4° (fig. 15, $c_l = 0.2$, $\delta_f = 0°$) as compared to an increment $\Delta\alpha_o$ of approximately 18° due to a total deflection of 40° (±20°) for a 0.20c conventional aileron. It is apparent, therefore, if equal rolling velocities are to be obtained, a spoiler aileron of the type tested should cover a larger portion of the wing semispan than a conventional aileron. This longer spoiler span is entirely feasible, however, because of the small wheel forces resulting from use of a spoiler of the type investigated.

Airfoil drag.- The effect of the total spoiler gap in the upper surface on the drag characteristics of the airfoil at a Reynolds number of 2.5 million is shown in figure 16. These results show that the section profile-drag coefficient was lowest with the 0.0141c spoiler total gap. The spanwise variation of the section profile-drag coefficient of the airfoil at a Reynolds number of 6 million with spoiler aileron configuration 9, which had a total gap of 0.0141c, is shown in figure 17. The peaks occurring in the drag-coefficient curves (figs. 16 and 17) at 5 inches either side of the center line appear to be caused by air flow in the chordwise slots in the airfoil upper surface. (See fig. 4.) Profile-drag-coefficient polars for different spoiler deflections are presented in figure 18. The section profile-drag coefficients presented in this figure were average values obtained from surveys over a 20-inch section of the model span as shown in figure 17. Because of the difficulties in making wake surveys behind the deflected spoiler, the profile-drag coefficients may be in error as much as 15 percent.

The effect of leakage of air in and out of the slots on the profile-drag coefficient of the airfoil with the spoiler retracted is shown in figure 19. It can be seen that the minimum profile-drag coefficient of the airfoil was increased approximately 12 percent by air flow.

Airfoil pitching moments.- The pitching-moment characteristics of the airfoil section at several spoiler aileron deflections are shown in figure 11. Because the change in pitching moment produced by lateral-control devices is of primary importance for determining the lateral-control reversal speed, figure 20 presents the increment in the pitching-moment coefficient $\Delta c_{m_{c/4}}$

based on the increment of section angle of attack produced by deflection of the spoiler aileron. A study of figure 20 shows that as the flap was deflected, the increment $\Delta c_{m_{c/4}}$ increased, and as the lift coefficient was increased, the increment decreased.

The increment $\Delta c_{m_{c/4}}$ at $c_l = 0$, for the same airfoil (NACA 66(215)-216) with a 0.20c sealed plain flap (reference 1) was included in figure 20 to judge the relative merits of the spoiler aileron and a plain sealed flap with respect to wing twist or lateral-control reversal speed. When a comparison is made at the same increment of section angle of attack, the increment of section pitching moment produced by the spoiler aileron is about 60 percent of the increment of section pitching moment produced by a 0.20c plain sealed flap or aileron. This agrees with the conclusion of reference 2 that the section pitching moments produced by spoiler ailerons were less positive than those produced by the plain flaps of equal effectiveness. The advantage of the smaller increments of section pitching moment associated with spoiler ailerons with respect to the lateral-control reversal speed of an airplane, however, may be offset by the relatively larger span required for spoiler ailerons.

CONCLUSIONS

The results of this investigation of a retractable spoiler aileron used as a lateral-control device on an NACA 66(215)-216 (approx.) airfoil section with a 0.25c slotted flap indicated the following conclusions:

1. The hinge-moment characteristics of the retractable spoiler aileron were greatly affected by spoiler thickness, rear-gap size, and bevel angle of the upper face of the spoiler. The best hinge-moment characteristics of the configurations tested were obtained with the thinnest (0.0028c) spoiler which had a 17° bevel angle on the upper and lower faces of the spoiler and roughness on the upper face, the largest (0.0100c) spoiler rear gap, and the 0.0013c spoiler forward gap.

2. The spoiler aileron was effective in producing a substantial decrease in the section lift coefficient for all negative spoiler deflections larger than -3°.

3. The spoiler effectiveness parameter $\Delta\alpha_o/\Delta\delta_s$ for deflections above -10° was practically unaffected by increasing the test Reynolds number from 2.5 to 6 million.

4. With the spoiler in the retracted position, air flow through the cut-outs for the spoiler in the upper surface of the airfoil caused an increase of approximately 12 percent in the minimum profile-drag coefficient.

5. The increments of section pitching-moment coefficient of the airfoil produced by the spoiler aileron were less positive than those produced by a plain sealed flap of equal effectiveness. The advantage of the smaller increments of section pitching moment associated with spoiler ailerons with respect to the lateral-control reversal speed of an airplane, however, may be offset by the relatively larger span required for spoiler ailerons.

Langley Memorial Aeronautical Laboratory
    National Advisory Committee for Aeronautics
        Langley Field, Va.

REFERENCES

1. Abbott, Ira H., von Doenhoff, Albert E., and Stivers,
      Louis S., Jr.: Summary of Airfoil Data. NACA
      ACR No. L5C05, 1945.

2. Purser, Paul E., and McKinney, Elizabeth G.: Com-
      parison of Pitching Moments Produced by Plain
      Flaps and by Spoilers and Some Aerodynamic Charac-
      teristics of an NACA 23012 Airfoil with Various
      Types of Aileron. NACA ACR No. L5C24a, 1945.
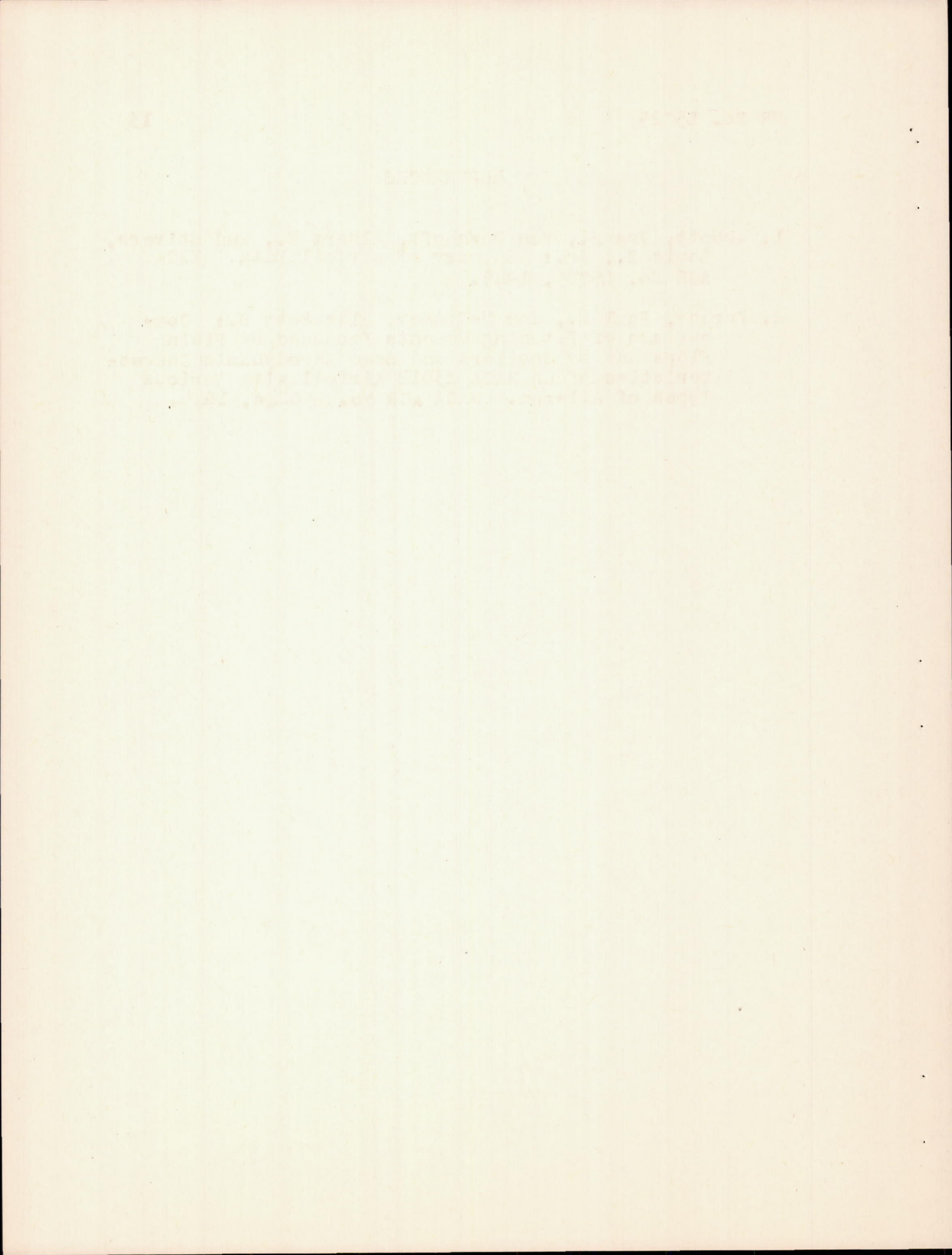
TABLE I

ORDINATES FOR THE SPOILER AILERON FLAP MODEL FOR THE HUGHES XF-11 AIRPLANE

[Stations and ordinates are given in percent of the airfoil chord]

Station	Airfoil		Flap slot		Flap	
	Upper airfoil ordinate	Lower airfoil ordinate	Upper slot ordinate	Lower slot ordinate	Upper flap ordinate	Lower flap ordinate
0	0	0				
0.50	1.324	1.024				
0.75	1.558	1.244				
1.25	1.921	1.563				
2.50	2.602	2.113				
5.00	3.621	2.894				
7.50	4.438	3.507				
10	5.126	4.022				
15.00	6.244	4.846				
20.00	7.112	5.481				
25.00	7.785	5.965				
30.00	8.297	6.337				
35.00	8.668	6.598				
40.00	8.906	6.762				
45.00	9.018	6.827				
50.00	8.993	6.785				
55.00	8.817	6.622				
60.00	8.437	6.287				
65.00	7.818	5.739				
70.00	6.954	4.982				
74.617	-----	4.138		1.456		
75.00	5.898	4.071	0.109	3.037		
75.625				T.E. Radius = 0.125		2.284
76.25	5.608		1.729		1.067	
77.50	5.313		2.678		2.142	
78.75	5.017		3.295		2.832	
80.00	4.714	3.084	3.660		3.293	3.084
81.25	4.400		3.833		3.557	
82.50	4.092		3.921		3.668	
83.125			T.E. Radius = 0.032			
83.75					3.634	
85.00					3.449	2.081
90.00					2.184	1.126
92.50					1.562	0.698
95.00					0.984	0.338
97.50					0.470	0.092
100.00					Trailing-edge radius 0.032	

NATIONAL ADVISORY
COMMITTEE FOR AERONAUTICS

TABLE II

DESCRIPTION OF VARIOUS TEST CONFIGURATIONS FOR THE SPOILER AILERON FLAP MODEL
FOR THE HUGHES XF-11 AIRPLANE

(See figures 2 and 3 for general arrangement.)

All dimensions unless otherwise noted are given in percent of airfoil chord

Configuration Number	Spoiler Thickness	Spoiler Forward Gap	Spoiler Rear Gap	Spoiler surface conditions
1	1.04	0.13	1.00	Both faces radial, no roughness.
2	1.04	0.13	0.77	Both faces radial, no roughness.
3	1.04	0.13	0.51	Both faces radial, no roughness.
4	1.04	0.13	0.24	Both faces radial, no roughness.
5	0.28	0.13	1.00	Spoiler beveled 30° on upper face, lower face radial, no roughness.
6	0.28	0.13	1.00	Spoiler beveled 10° on upper face, beveled 17° on the lower face, no roughness.
7	0.28	0.13	1.00	Spoiler beveled 10° on upper face, beveled 17° on the lower face, roughness on upper face.
8	0.28	0.13	1.00	Spoiler beveled 17° on both faces, no roughness.
9	0.28	0.13	1.00	Spoiler beveled 17° on both faces, roughness on upper face.

NATIONAL ADVISORY
COMMITTEE FOR AERONAUTICS.

TABLE III

SPOILER SURFACE AND CHAMBER PRESSURES FOR THE SPOILER AILERON FLAP MODEL FOR THE HUGHES XF-11 AIRPLANE
(For location of pressure tubes see figures 3 and 5.)

(Configuration number 1; Reynolds number = 2.50×10^6; Mach number = 0.18)

| Tube numbers →			1	2	3	4	5	6	7	8	9	10	11	12	13	14	15	16	17	18	19	20	21
Test conditions																							
α_0 (deg)	δ_s (deg)	δ_f (deg)								Pressure coefficient, S													
0	0	0	0.972	0.821	0.792	1.307	1.297	1.287	1.285	1.287	1.287	1.293	1.297	1.297	1.293	1.292	1.292	1.292	1.292	1.292	1.285	1.311	1.291
0	-10	0	1.068	1.006	1.020	0.781	1.245	1.231	1.185	1.163	1.156	1.155	1.158	1.158	1.163	1.170	1.175	1.175	1.170	1.123	1.252	1.163
0	-20	0	1.146	1.106	1.348	0.374	0.468	1.321	1.330	1.330	1.257	1.259	1.255	1.273	1.287	1.283	1.287	1.287	1.278	1.267	1.195	1.356	1.275
0	-30	0	1.126	1.066	1.345	0.272	0.364	0.376	1.090	1.408	1.456	1.311	1.328	1.330	1.341	1.354	1.355	1.345	1.328	1.311	1.241	1.422	1.331
0	-40	0	1.047	0.925	1.131	0.209	0.298	0.326	0.328	0.362	1.571	1.320	1.354	1.355	1.405	1.400	1.496	1.376	1.354	1.340	1.238	1.507	1.361
0	-45	0	1.018	0.867	0.996	0.201	0.282	0.310	0.314	0.308	0.568	1.543	1.671	1.670	1.420	1.410	1.408	1.400	1.382	1.368	1.253	1.304	1.322
0	-52	0	0.970	0.791	0.817	0.193	0.266	0.292	0.304	0.312	0.324	1.493	1.484	1.478	1.448	1.444	1.437	1.421	1.403	1.398	1.178	1.203	1.106
2.03	-52	0	0.958	0.774	0.718	0.243	0.316	0.338	0.350	0.352	0.362	1.476	1.468	1.465	1.440	1.446	1.444	1.430	1.420	1.405	1.166	1.195	1.096
4.06	-52	0	0.957	0.772	0.672	0.340	0.400	0.414	0.417	0.417	0.429	1.494	1.485	1.470	1.452	1.455	1.452	1.442	1.426	1.420	1.196	1.221	1.110
6.08	0	0	1.187	1.135	1.098	1.285	1.284	1.280	1.277	1.277	1.244	1.280	1.280	1.280	1.277	1.277	1.280	1.280	1.277	1.280	1.279	1.287	1.281
6.08	-10	0	1.106	1.055	1.022	0.919	1.227	1.228	1.206	1.123	1.192	1.189	1.191	1.193	1.197	1.199	1.201	1.201	1.203	1.199	1.179	1.231	1.204
6.08	-20	0	1.115	1.022	0.976	0.680	0.718	0.555	1.316	1.328	1.277	1.244	1.268	1.280	1.290	1.287	1.292	1.293	1.287	1.280	1.227	1.340	1.284
6.08	-30	0	1.094	0.978	0.925	0.549	0.604	0.595	0.894	1.408	1.450	1.337	1.350	1.354	1.357	1.368	1.368	1.360	1.348	1.334	1.271	1.428	1.348
6.08	-40	0	1.030	0.861	0.808	0.467	0.531	0.539	0.531	0.549	1.555	1.345	1.376	1.373	1.412	1.408	1.400	1.385	1.365	1.355	1.271	1.505	1.371
6.08	-45	0	1.004	0.847	0.768	0.461	0.513	0.519	0.531	0.507	0.610	1.574	1.626	1.600	1.436	1.430	1.425	1.415	1.400	1.387	1.307	1.328	1.315
6.08	-52	0	0.948	0.758	0.664	0.423	0.475	0.485	0.487	0.483	0.487	1.490	1.486	1.485	1.456	1.458	1.456	1.444	1.430	1.428	1.221	1.243	1.116
8.12	-52	0	0.851	0.640	0.527	0.576	0.632	0.640	0.636	0.628	0.612	1.480	1.476	1.460	1.455	1.448	1.438	1.415	1.418	1.415	1.241	1.261	1.195
9.14	0	0	1.215	1.197	1.198	1.238	1.238	1.238	1.238	1.238	1.238	1.240	1.240	1.240	1.240	1.240	1.240	1.240	1.240	1.249	1.243	1.240	1.219
9.14	-10	0	1.140	1.108	1.098	1.078	1.203	1.195	1.187	1.183	1.181	1.183	1.183	1.185	1.185	1.185	1.187	1.187	1.187	1.185	1.180	1.207	1.187
9.14	-20	0	1.141	1.084	1.054	0.957	0.971	1.287	1.289	1.283	1.255	1.257	1.255	1.269	1.275	1.277	1.277	1.273	1.267	1.237	1.299	1.273
9.14	-30	0	1.110	1.013	0.968	0.872	0.895	0.889	1.190	1.365	1.388	1.315	1.323	1.331	1.337	1.343	1.345	1.343	1.333	1.325	1.283	1.382	1.329
9.14	-40	0	1.042	0.917	0.856	0.806	0.836	0.834	0.826	0.836	1.476	1.347	1.369	1.365	1.385	1.384	1.382	1.375	1.362	1.355	1.295	1.454	1.359
9.14	-45	0	1.006	0.873	0.806	0.782	0.808	0.808	0.802	0.786	0.893	1.478	1.524	1.514	1.403	1.399	1.397	1.392	1.382	1.373	1.313	1.323	1.321
9.14	-52	0	0.921	0.758	0.688	0.734	0.762	0.764	0.760	0.752	0.742	1.464	1.462	1.458	1.436	1.432	1.424	1.416	1.407	1.407	1.255	1.277	1.231
10.15	-52	0	1.306	0.805	0.732	0.798	0.825	0.825	0.821	0.812	0.805	1.455	1.453	1.448	1.424	1.423	1.416	1.507	1.402	1.402	1.267	1.284	1.221
12.18	-52	0	0.998	0.889	0.837	0.925	0.942	0.940	0.934	0.922	0.912	1.450	1.448	1.448	1.418	1.416	1.507	1.400	1.396	1.397	1.287	1.300	1.255
9.14	0	20	1.548	1.560	1.592	1.588	1.592	1.592	1.592	1.592	1.592	1.588	1.590	1.592	1.592	1.592	1.592	1.594	1.594	1.609	1.594	1.588	1.601
9.14	-10	20	1.384	1.350	1.327	1.317	1.472	1.463	1.451	1.445	1.445	1.447	1.447	1.447	1.447	1.447	1.447	1.448	1.447	1.443	1.474	1.453
9.14	-20	20	1.357	1.293	1.255	1.143	1.167	1.508	1.514	1.506	1.476	1.487	1.485	1.493	1.500	1.500	1.504	1.497	1.491	1.462	1.521	1.499
9.14	-30	20	1.230	1.198	1.148	1.053	1.077	1.068	1.396	1.576	1.597	1.528	1.538	1.540	1.546	1.552	1.554	1.552	1.542	1.533	1.487	1.590	1.538
9.14	-40	20	1.212	1.091	1.023	0.990	1.018	1.013	1.003	1.008	1.679	1.561	1.582	1.576	1.594	1.593	1.590	1.582	1.567	1.558	1.489	1.655	1.548
9.14	-45	20	1.179	1.052	0.986	0.969	0.992	0.990	0.977	0.960	1.078	1.678	1.710	1.689	1.597	1.592	1.590	1.586	1.573	1.565	1.506	1.514	1.512
9.14	-52	20	1.096	0.946	0.876	0.929	0.952	0.952	0.943	0.935	0.927	1.672	1.670	1.670	1.634	1.622	1.604	1.592	1.586	1.583	1.452	1.466	1.422
-10.15	-52	40	1.126	0.978	1.170	0.193	0.235	0.250	0.259	0.265	0.290	1.705	1.690	1.685	1.660	1.660	1.636	1.606	1.590	1.582	1.316	1.350	1.258
-8.12	-52	40	1.163	1.006	1.150	0.225	0.263	0.281	0.290	0.294	0.316	1.745	1.735	1.724	1.702	1.681	1.650	1.625	1.615	1.605	1.354	1.383	1.275
-6.08	-52	40	1.380	1.017	1.114	0.241	0.288	0.307	0.318	0.320	0.340	1.797	1.786	1.785	1.750	1.738	1.713	1.690	1.675	1.665	1.405	1.430	1.275
-4.06	-52	40	1.180	0.979	1.018	0.249	0.319	0.340	0.354	0.358	0.377	1.818	1.807	1.805	1.767	1.772	1.755	1.726	1.710	1.698	1.414	1.415	1.344
4.06	-10	40	1.710	1.622	1.565	1.613	1.944	1.931	1.896	1.876	1.870	1.862	1.864	1.870	1.878	1.883	1.887	1.892	1.893	1.887	1.847	1.946	1.849
4.06	-20	40	1.420	1.317	1.295	1.082	1.123	1.166	1.177	1.170	1.127	1.136	1.133	1.125	1.125	1.127	1.128	1.132	1.132	1.127	1.539	1.621	1.578
4.06	-30	40	1.323	1.199	1.137	0.957	0.992	0.980	1.609	1.670	1.698	1.609	1.614	1.616	1.605	1.609	1.606	1.605	1.595	1.553	1.691	1.607
4.06	-45	40	1.717	1.054	0.968	0.865	0.902	0.902	0.889	0.870	1.223	1.815	1.852	1.857	1.774	1.766	1.769	1.769	1.761	1.749	1.607	1.636	1.633
4.06	-52	40	1.136	0.911	0.805	0.793	0.835	0.840	0.837	0.827	0.825	1.900	1.893	1.895	1.833	1.836	1.816	1.796	1.785	1.783	1.579	1.585	1.541
8.12	-52	40	1.724	1.068	0.992	1.051	1.073	1.078	1.071	1.063	1.056	1.875	1.874	1.870	1.826	1.820	1.602	1.790	1.783	1.777	1.635	1.647	1.596
10.15	0	40	1.891	1.885	1.942	1.960	1.960	1.960	1.960	1.960	1.960	1.960	1.962	1.962	1.962	1.962	1.962	1.962	1.962	1.966	1.962	1.958	1.969
10.15	-10	40	1.577	1.551	1.538	1.535	1.655	1.641	1.633	1.630	1.630	1.630	1.630	1.630	1.630	1.639	1.630	1.630	1.632	1.628	1.621	1.663	1.637
10.15	-20	40	1.431	1.394	1.372	1.347	1.345	1.546	1.551	1.540	1.524	1.522	1.522	1.524	1.524	1.526	1.531	1.531	1.533	1.531	1.508	1.559	1.531
10.15	-30	40	1.437	1.363	1.327	1.284	1.301	1.287	1.569	1.512	1.662	1.617	1.619	1.614	1.614	1.617	1.614	1.614	1.617	1.600	1.676	1.626
10.15	-40	40	1.387	1.283	1.233	1.243	1.263	1.258	1.236	1.233	1.794	1.703	1.710	1.708	1.703	1.700	1.698	1.695	1.688	1.680	1.647	1.776	1.668
10.15	-45	40	1.328	1.215	1.162	1.195	1.218	1.215	1.203	1.183	1.319	1.693	1.703	1.705	1.708	1.705	1.703	1.698	1.695	1.685	1.622	1.743	1.668
10.15	-52	40	1.276	1.137	1.072	1.173	1.195	1.195	1.190	1.183	1.175	1.895	1.902	1.913	1.847	1.847	1.837	1.819	1.809	1.806	1.645	1.657	1.642
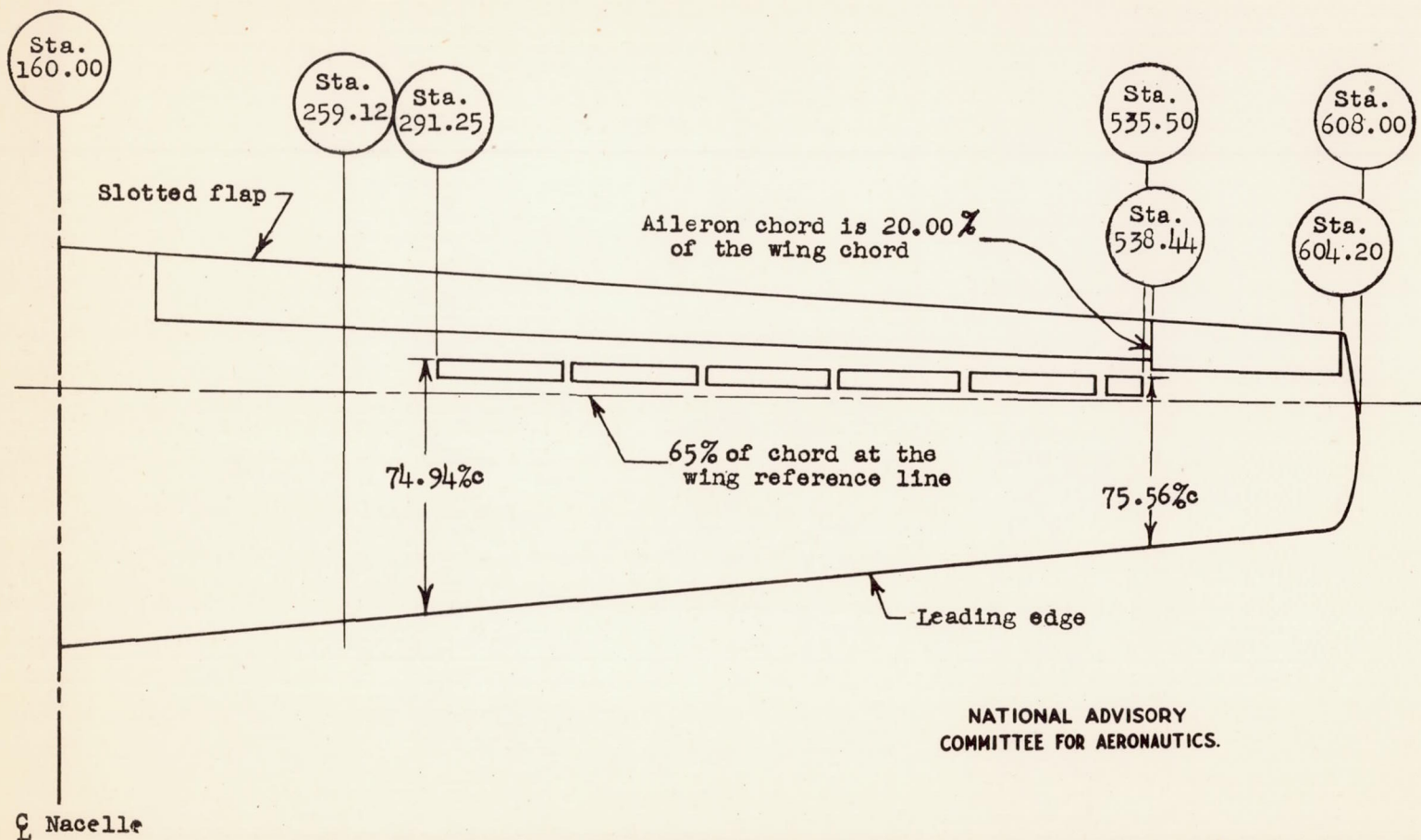
Figure 1.- Schematic drawing of the lefthand outboard wing panel for the Hughes XF-11 airplane showing the aileron and spoilers.
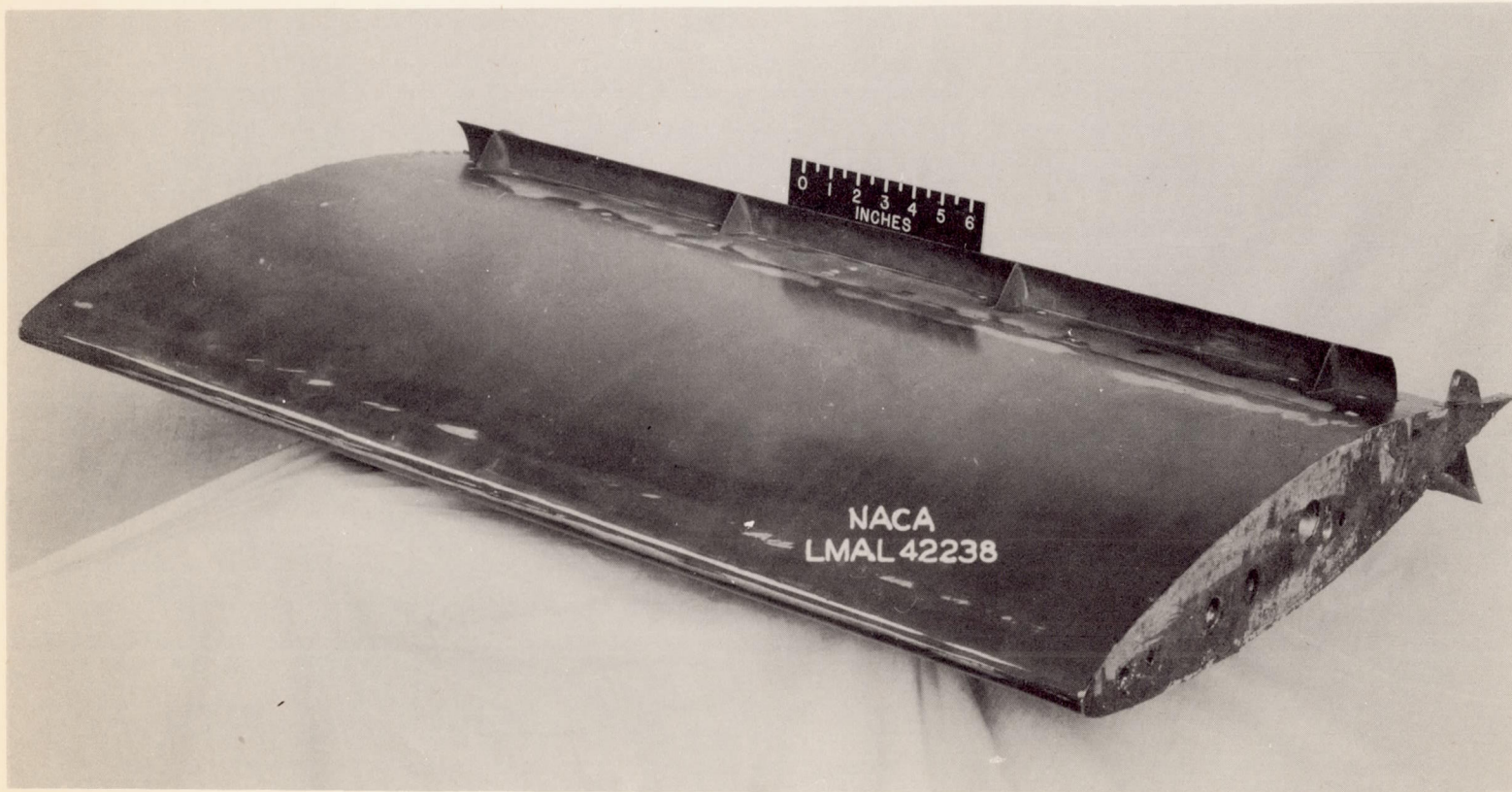
(a) Three-quarter front view of model showing the spoiler webs.

Figure 2.- Photographs showing the spoiler arrangement and the chordwise slots in the airfoil upper surface for the spoiler webs. Spoiler aileron flap model for the Hughes XF-11 airplane.
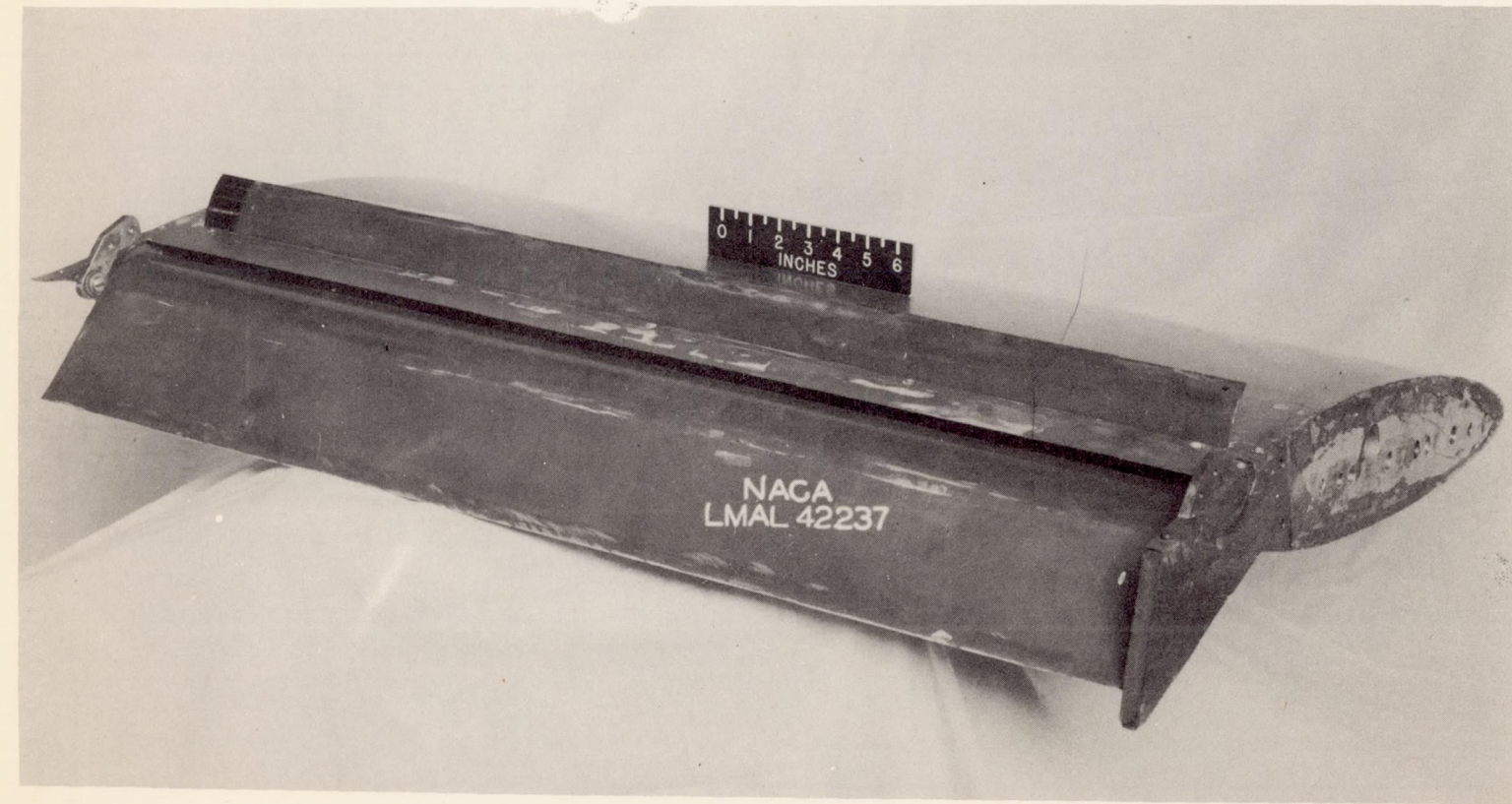
(b)   Three-quarter rear view of model showing the spoiler aileron and slotted flap deflected.

Figure 2.- Continued.

(c) Three-quarter top view of model showing the spoiler aileron slots in the airfoil
upper surface.

Figure 2.- Concluded.

Spoiler webs are located 5.031 and 14.967 inches either side of the model centerline.

The spoiler deflection is measured from airfoil upper surface to the upper face of spoiler; the sign is negative for spoiler deflections above airfoil surface and is positive for deflections below airfoil upper surface.

−52°

+3°

0.0531

0°

20°

0.664

40°

0.25

1.000

Airfoil chord, 24.00 in.
Spoiler span, 33.44 in.

10, 17, and 30 degree bevels were cut on the 0.28-percent chord thick spoiler

10° 17° 30°

Carborundum roughness was applied to this face of the spoiler aileron

All dimensions are given in fractions of the airfoil chord unless otherwise noted

Gap dimensions	
Front gap B	Rear gap C
0.0013	0.0100
.0013	.0077
.0013	.0051
.0013	.0024

Spoiler aileron dimensions	
Thickness t	Mean radius R_m
0.0104	0.0843
.0028	.0881

B

C

20 21

19

Spoiler chamber orifices

0.0896

R_m

17°

t

NATIONAL ADVISORY
COMMITTEE FOR AERONAUTICS.

Figure 3.- Sketch showing the general model arrangement, spoiler, and spoiler slot details for the spoiler aileron flap model for the Hughes XF-11 airplane.

.0141

Spoiler removed

.0052

.4193 Distance between inboard slots

.0814

All dimensions are given in
fractions of the airfoil chord

NATIONAL ADVISORY
COMMITTEE FOR AERONAUTICS.
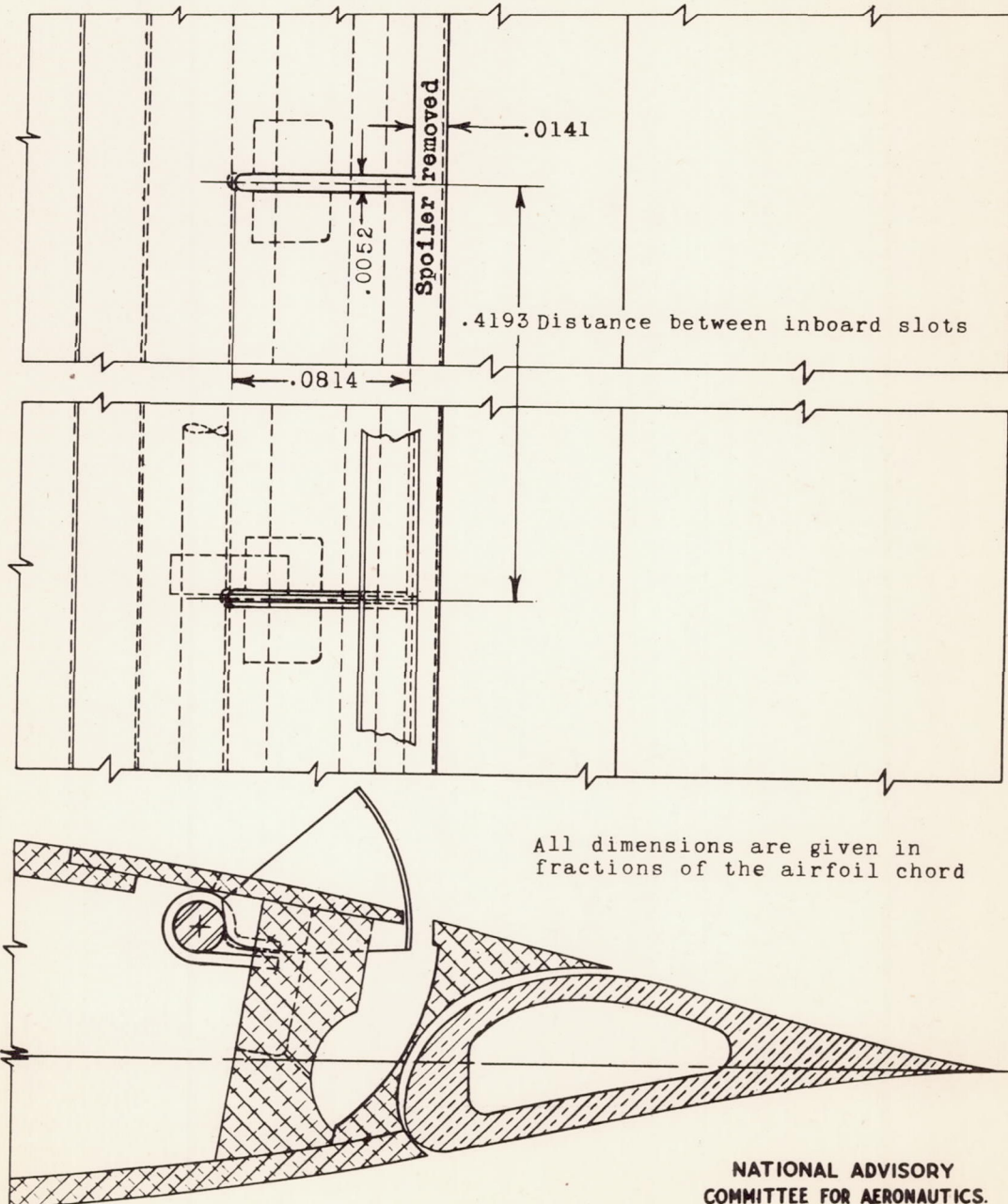
Figure 4.- Sketch showing the chordwise slots in the airfoil upper surface
for the spoiler webs for the 0.28-percent airfoil chord spoiler. Spoiler
aileron flap model for the Hughes XF-11 airplane.

Orifices 19, 20, and 21 are in
spoiler slot and are shown
in figure 3.

All dimensions are given
in inches and were measured
along each surface.

0.115   0.055

.235 .170

1.550

.215

.490

.705

.919

1.585

1.130

1.360

1.270

1.032

1.820

.785

.540

.240

.165

2.35

0.125

0.075
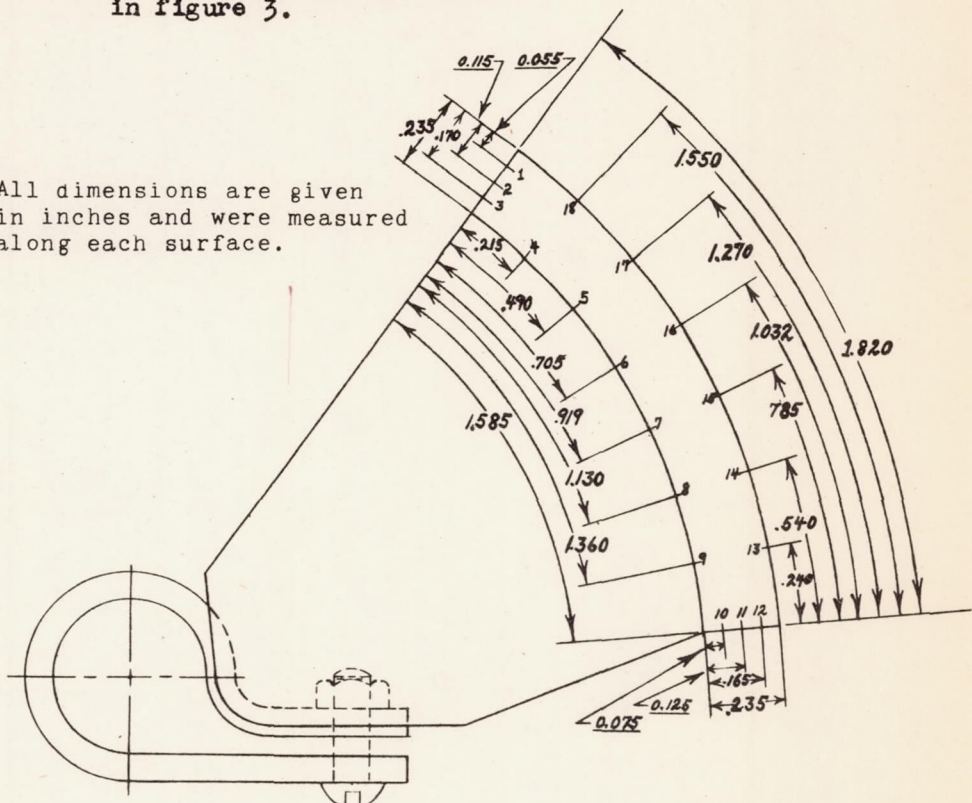
Figure 5.- Sketch showing the location of the pressure orifices in the
1.04-percent airfoil chord spoiler for the spoiler aileron flap model
for the Hughes XF-11 airplane.

NATIONAL ADVISORY
COMMITTEE FOR AERONAUTICS.
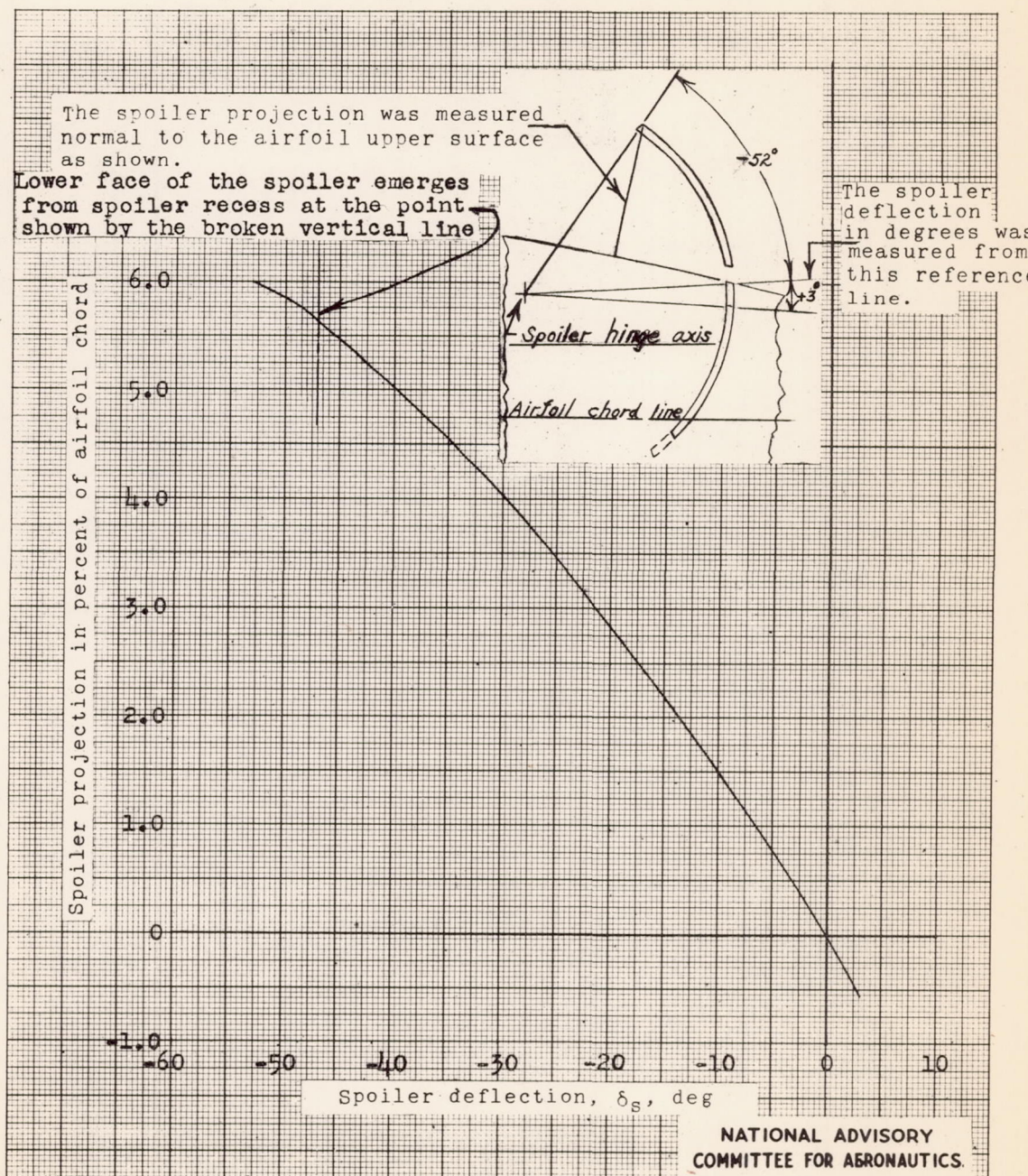
Figure 6.- Variation of spoiler projection in percent of airfoil chord with spoiler deflection in degrees for the spoiler aileron flap model for the Hughes XF-11 airplane.

δ_f (deg)	Configuration No.	Spoiler rear gap dimension (percent airfoil chord)
0	1	1.00
0	2	.77
0	3	.51
0	4	.24

NATIONAL ADVISORY
COMMITTEE FOR AERONAUTICS.

(a) $a_o = 0°$.
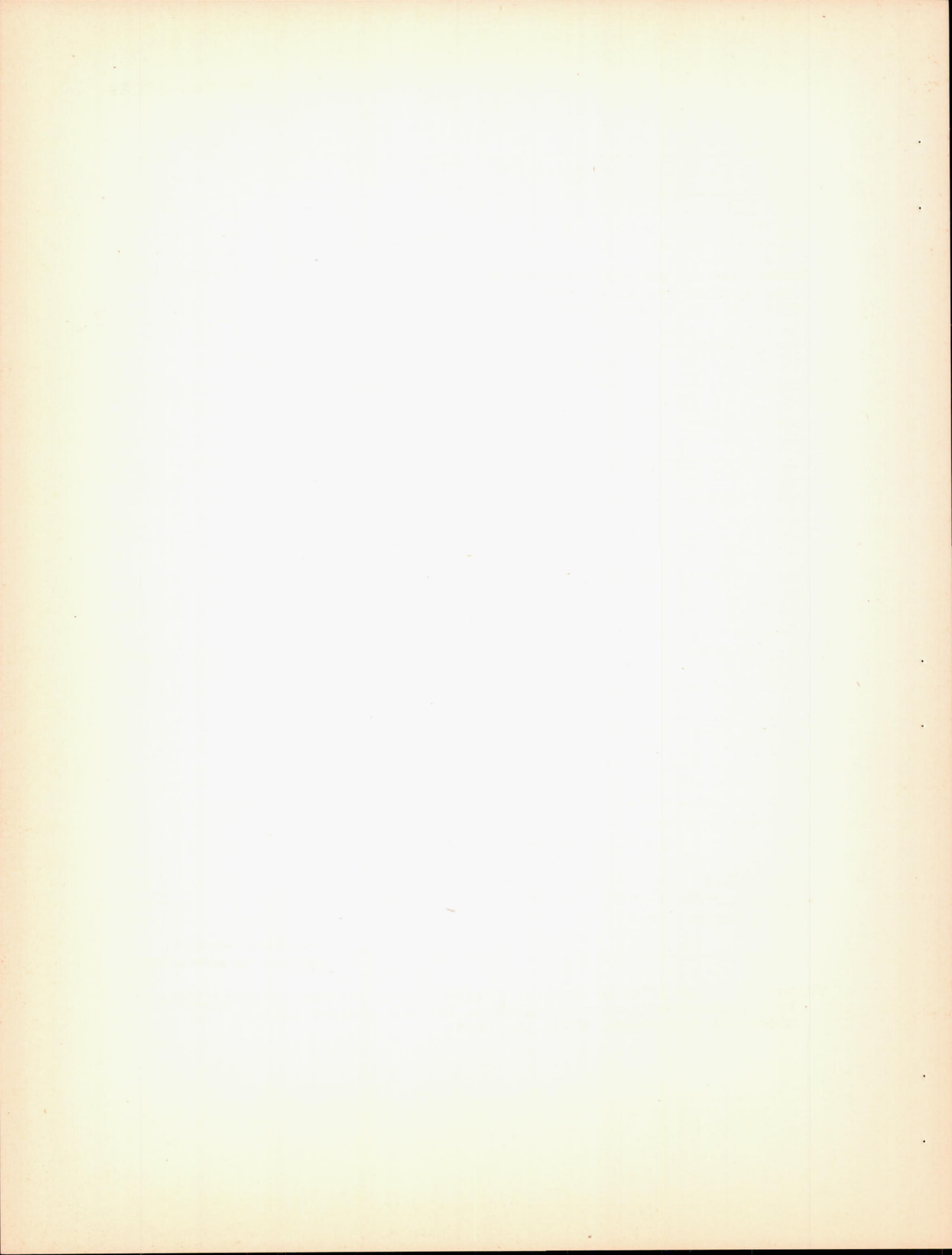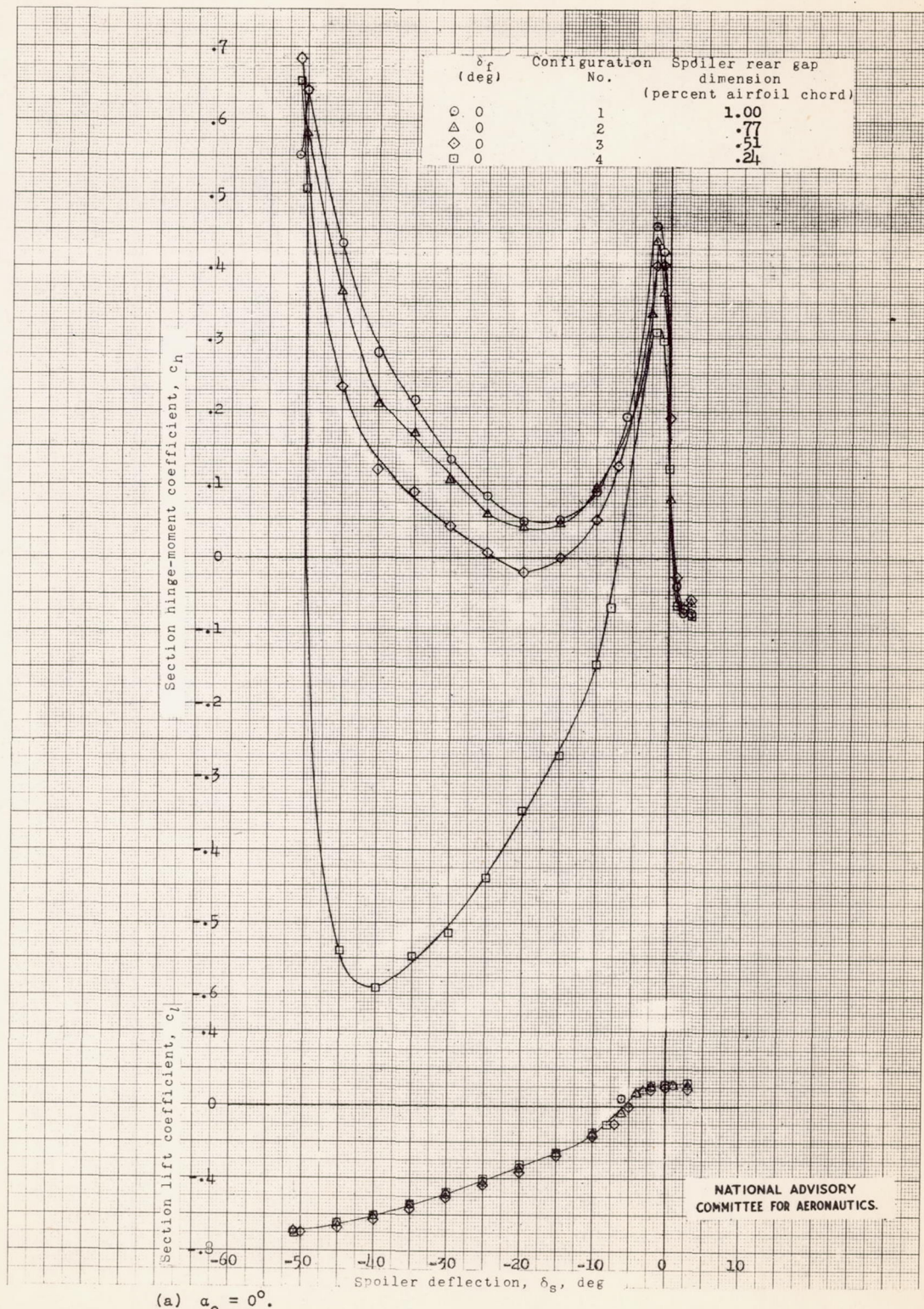
Figure 7.- Variation of section hinge-moment and lift coefficient with spoiler rear gap dimension for the spoiler aileron flap model for the Hughes XF-11 airplane. $R = 2.5 \times 10^6$; LTT test 392.

| δ_f (deg)	Configuration No.	Spoiler rear gap dimension (percent airfoil chord)
0	1	1.00
40	1	1.00
0	3	.51
40	3	.51

NATIONAL ADVISORY
COMMITTEE FOR AERONÁUTICS.

Section hinge-moment coefficient, c_h

Section lift coefficient, c_l

Spoiler deflection, δ_s, deg

Spoiler deflection, δ_s, deg

(b) $\alpha_o = 7.11°$.

Figure 7.- Concluded.
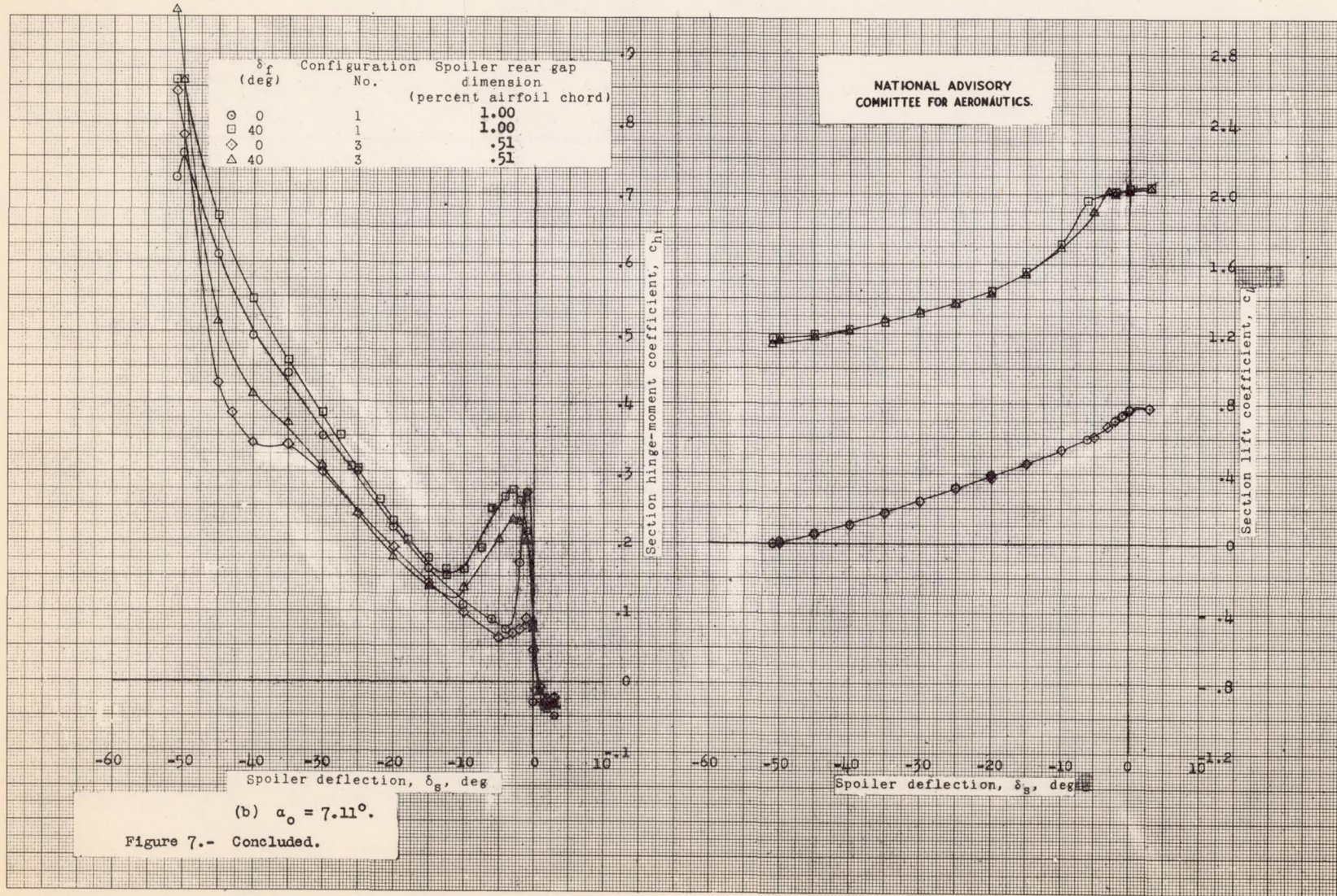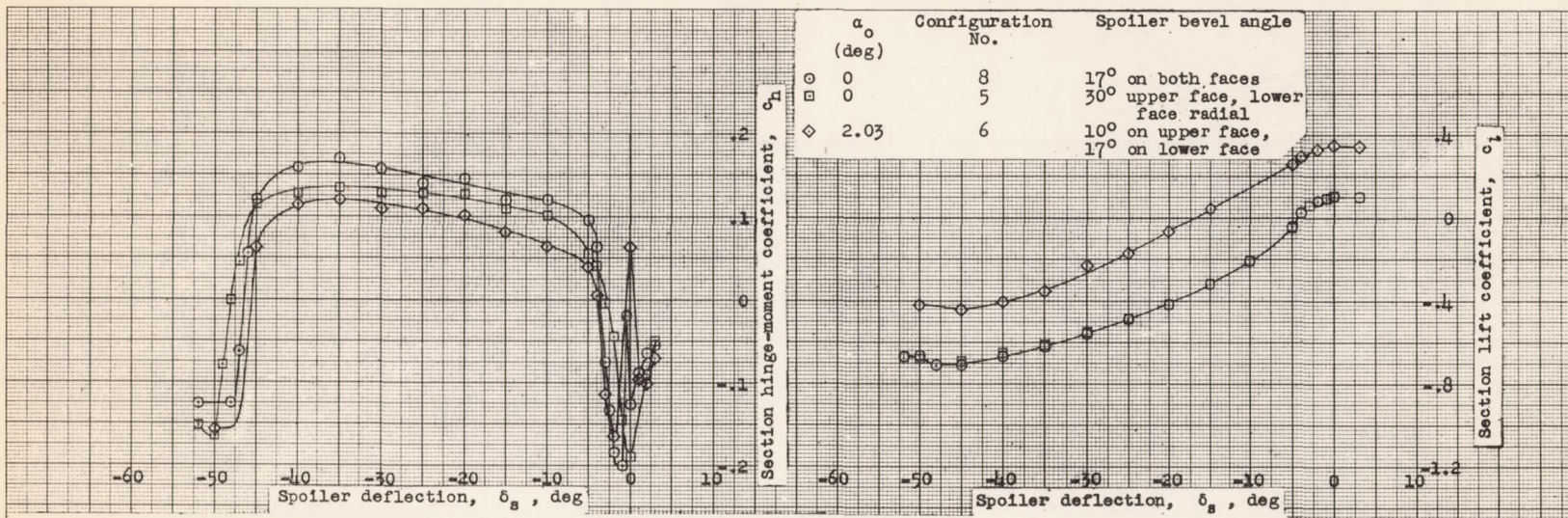
Figure 8.— The effect of spoiler bevel angle on the section hinge-moment and lift characteristics of the spoiler aileron flap model for the Hughes XF-11 airplane. Spoiler upper face smooth; $\delta_f = 0°$; $R = 2.5 \times 10^6$; LTT test 392.
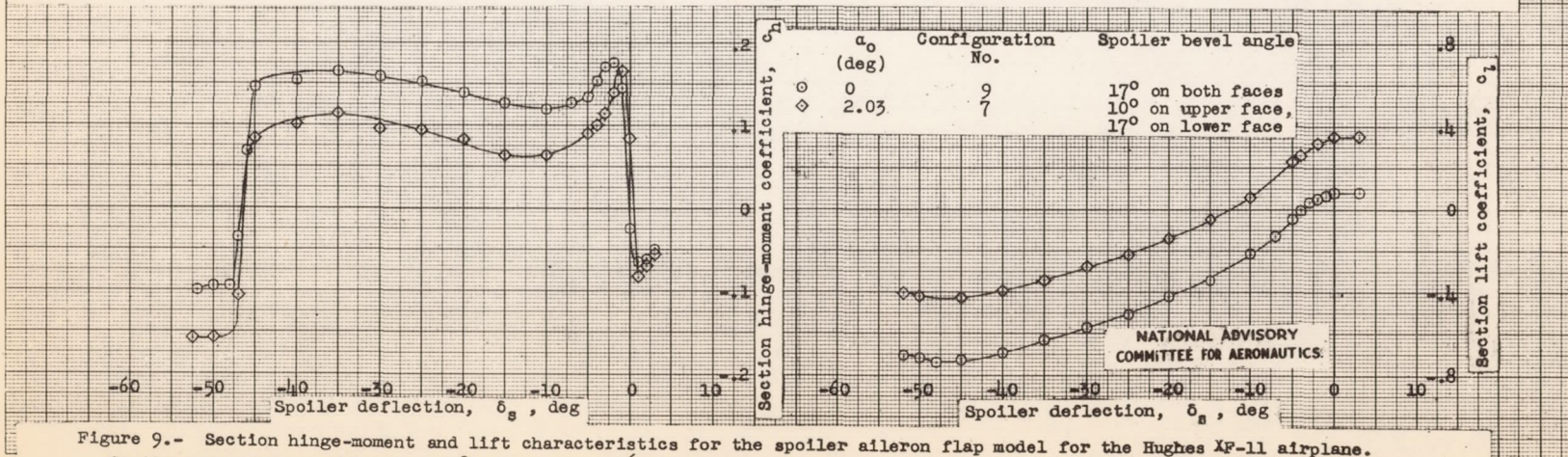
Figure 9.— Section hinge-moment and lift characteristics for the spoiler aileron flap model for the Hughes XF-11 airplane. Spoiler upper face rough; $\delta_f = 0°$; $R = 2.5 \times 10^6$; LTT test 392.
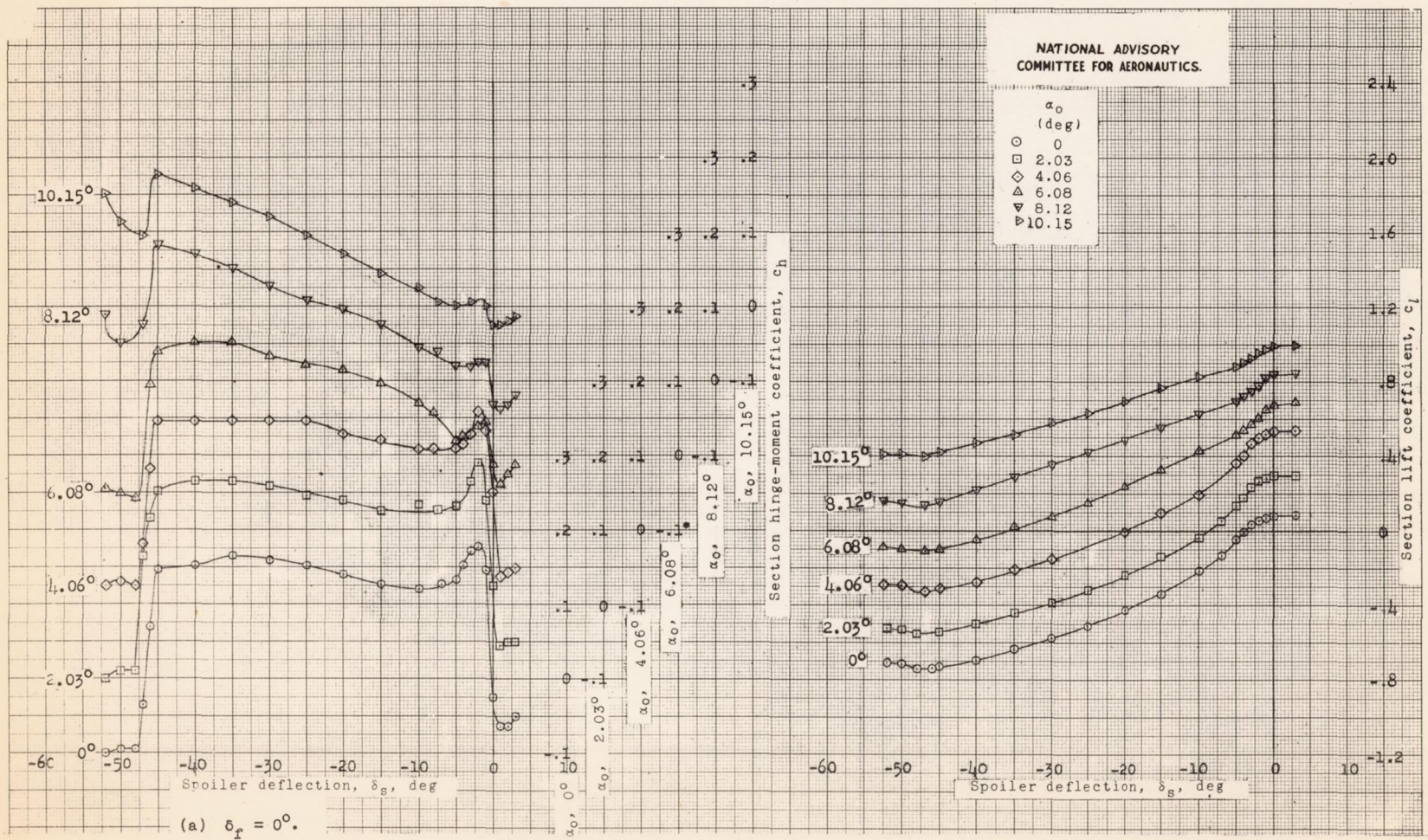
Figure 10.- Section hinge-moment and lift characteristics for the spoiler aileron flap model for the Hughes XF-11 airplane. Configuration number 9; R = 2.5 × 10⁶; LTT test 393.

(b) $\delta_f = 20°$.

Figure 10.- Continued.

(c) $\delta_f = 40°$.

Figure 10.- Concluded.

NATIONAL ADVISORY
COMMITTEE FOR AERONAUTICS.

Section lift coefficient, c_l

δ_s
(deg)

⊙ 3
□ -3
◇ -10
△ -20
▽ -30
▷ -45

Section pitching-moment coefficient $c_{m_{c/4}}$

Section angle of attack, α_0, deg

(a) $\delta_f = 0°$.
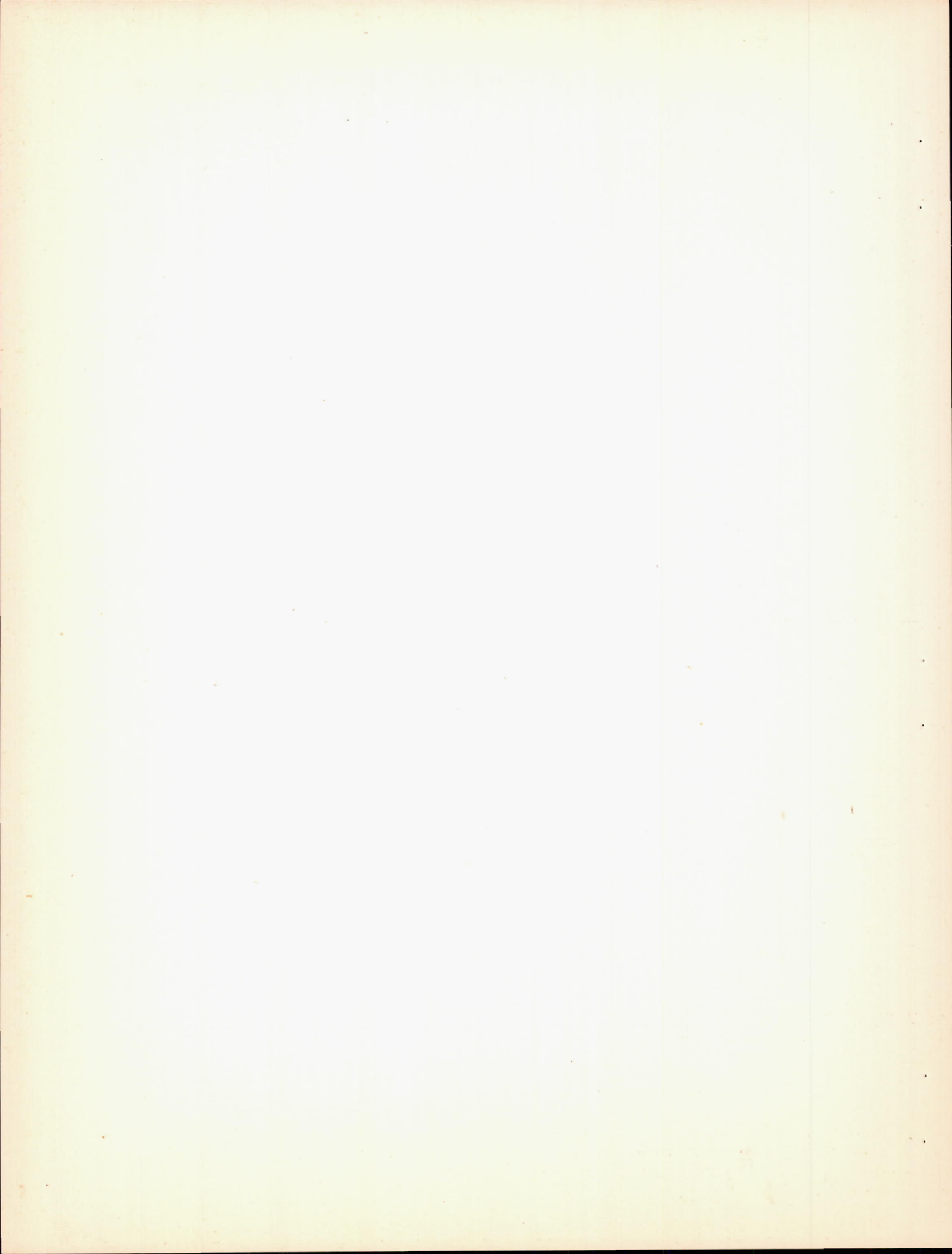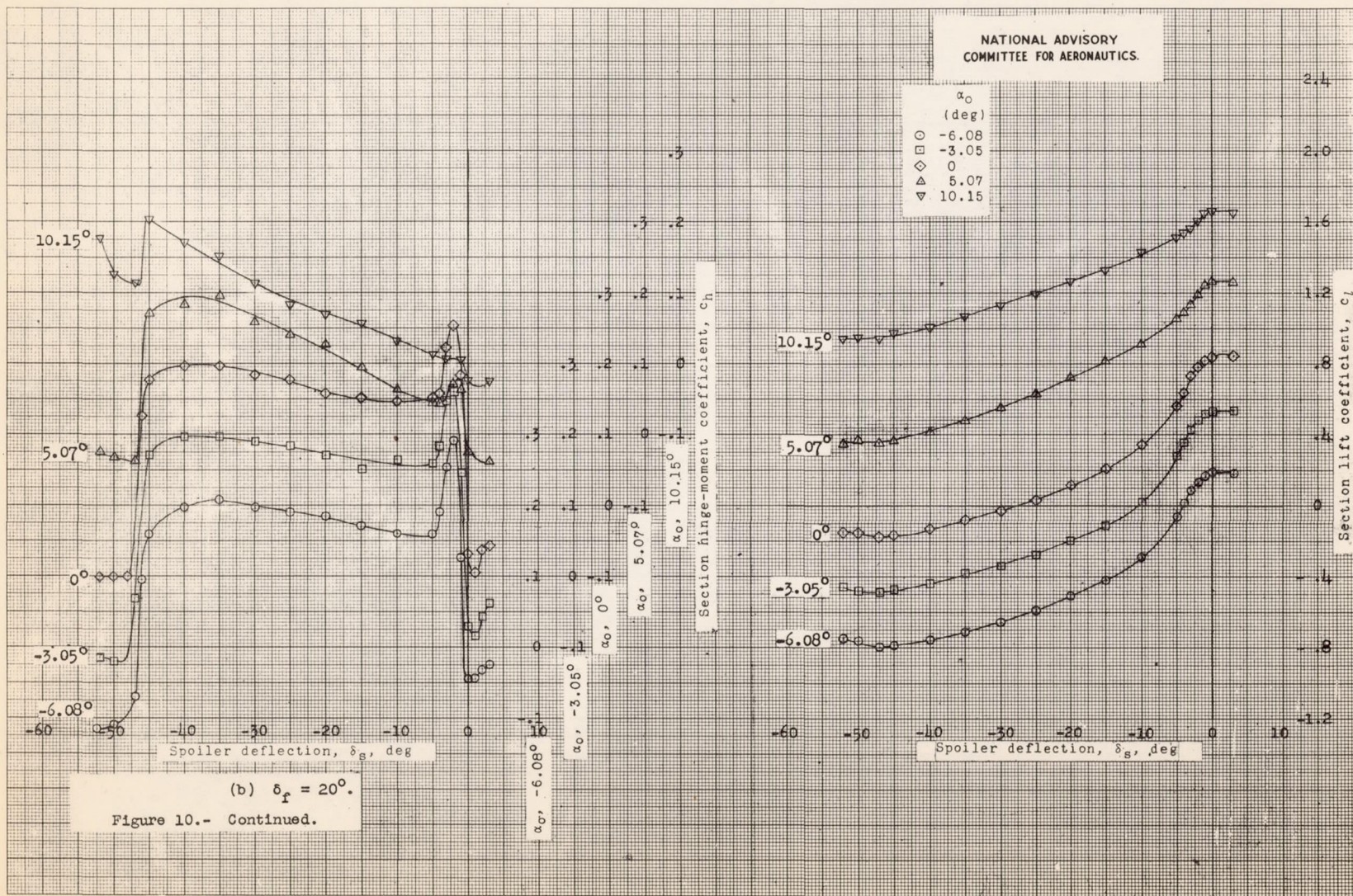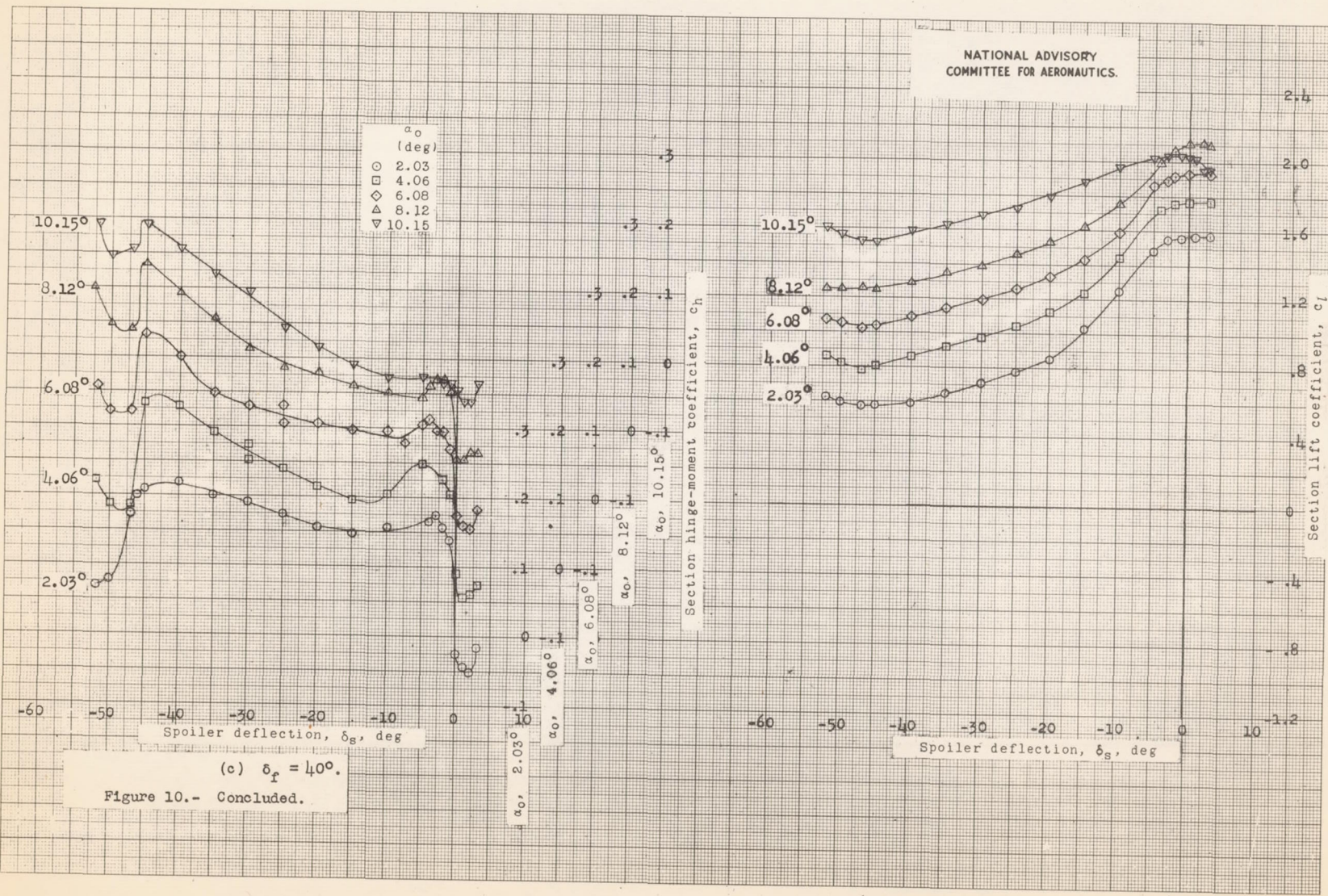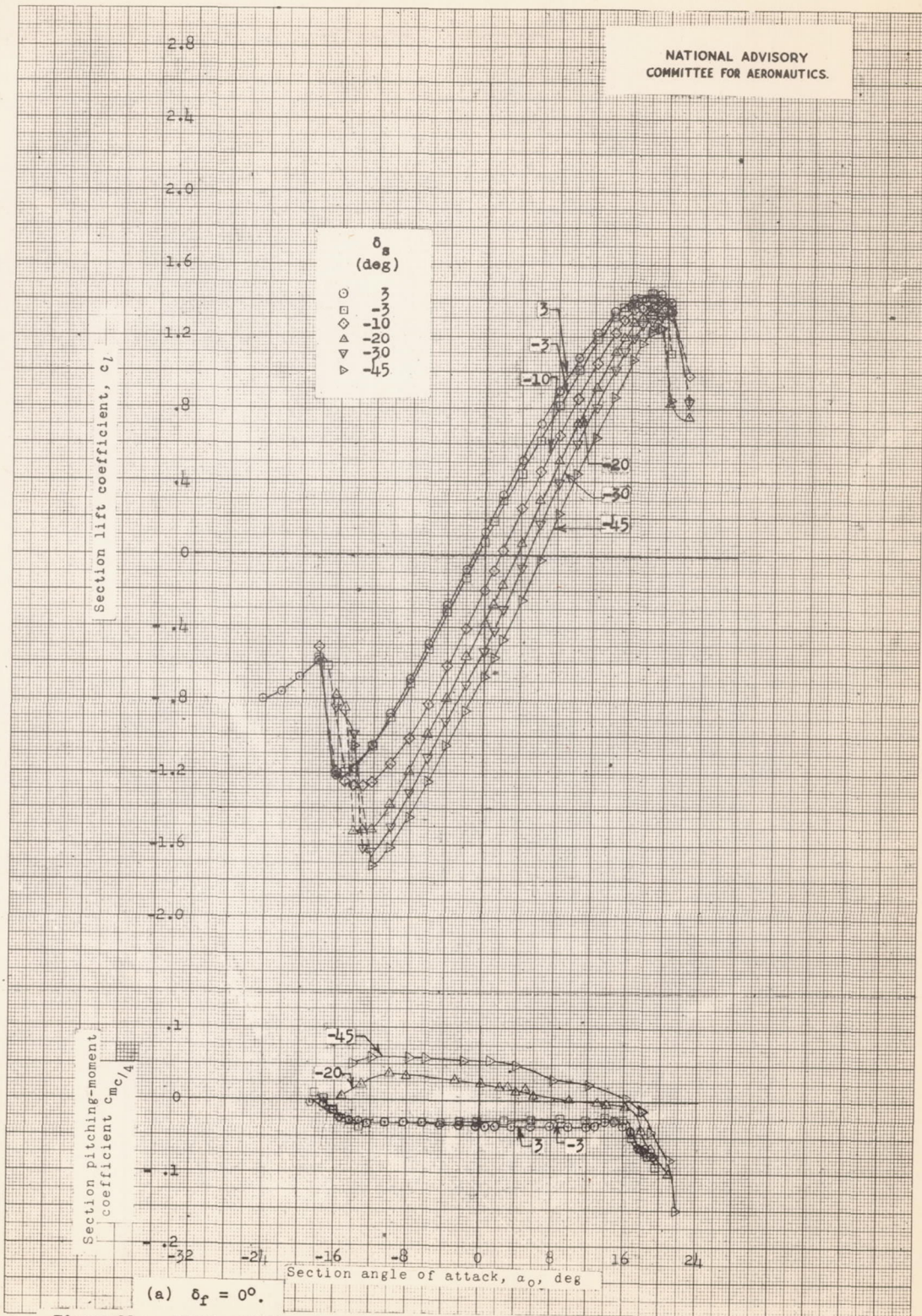
Figure 11.- Section lift and pitching-moment characteristics for the spoiler aileron flap model for the Hughes XF-11 airplane. Configuration number 9; $R = 6.0 \times 10^6$; TDT tests 799 and 800.

(b) $\delta_f = 20°$.

Figure 11.- Continued.

(c) $\delta_f = 40°$.

Figure 11.- Concluded.
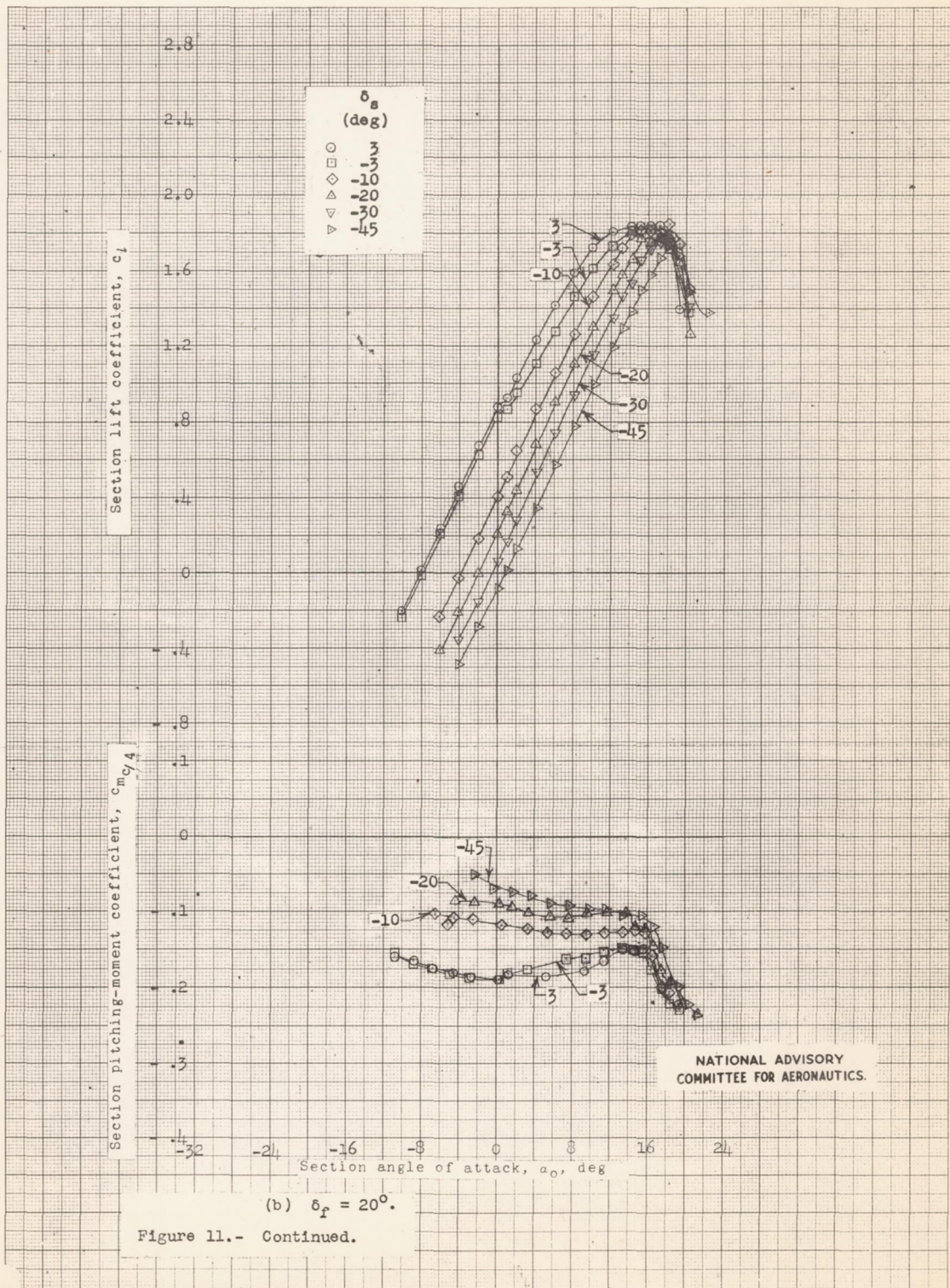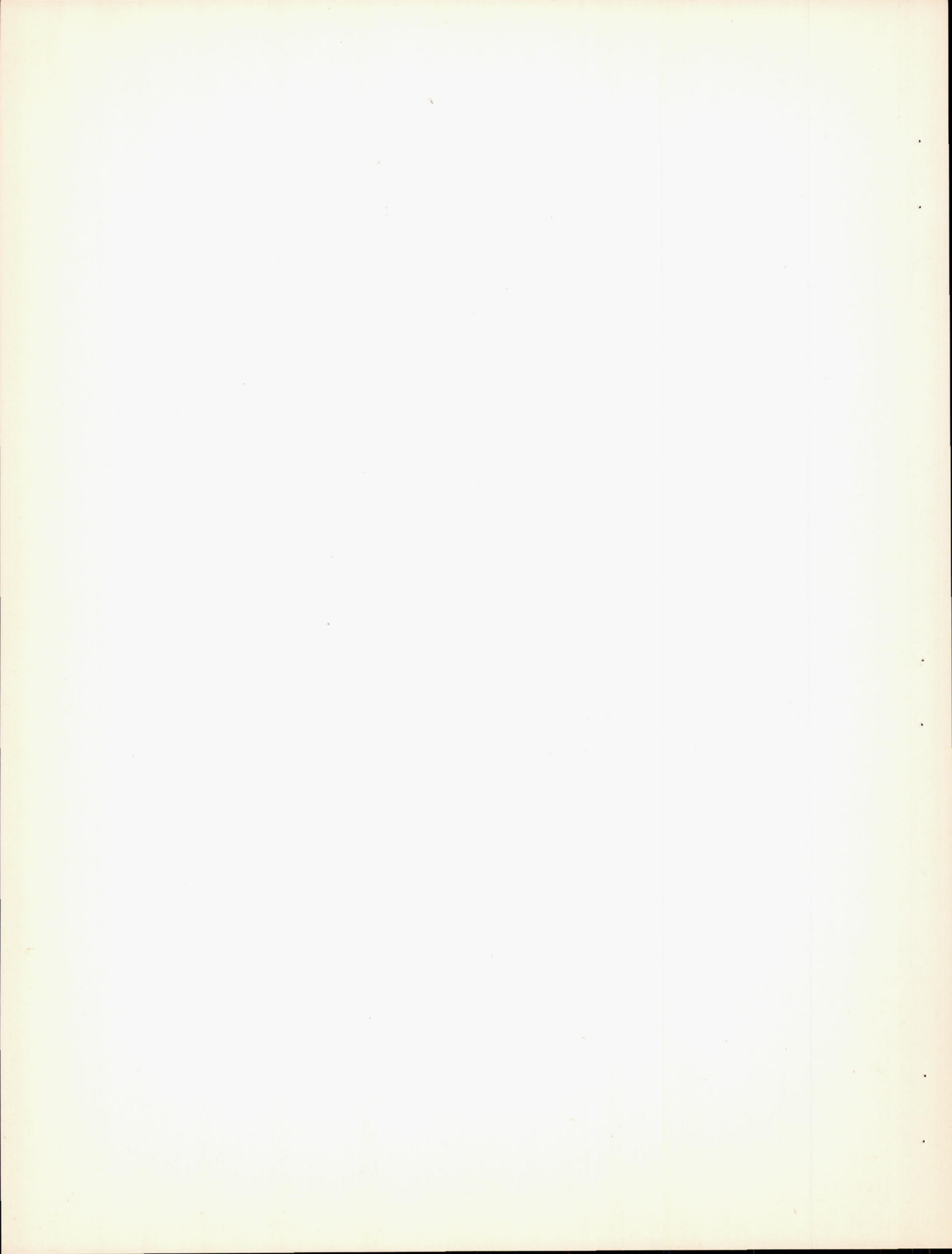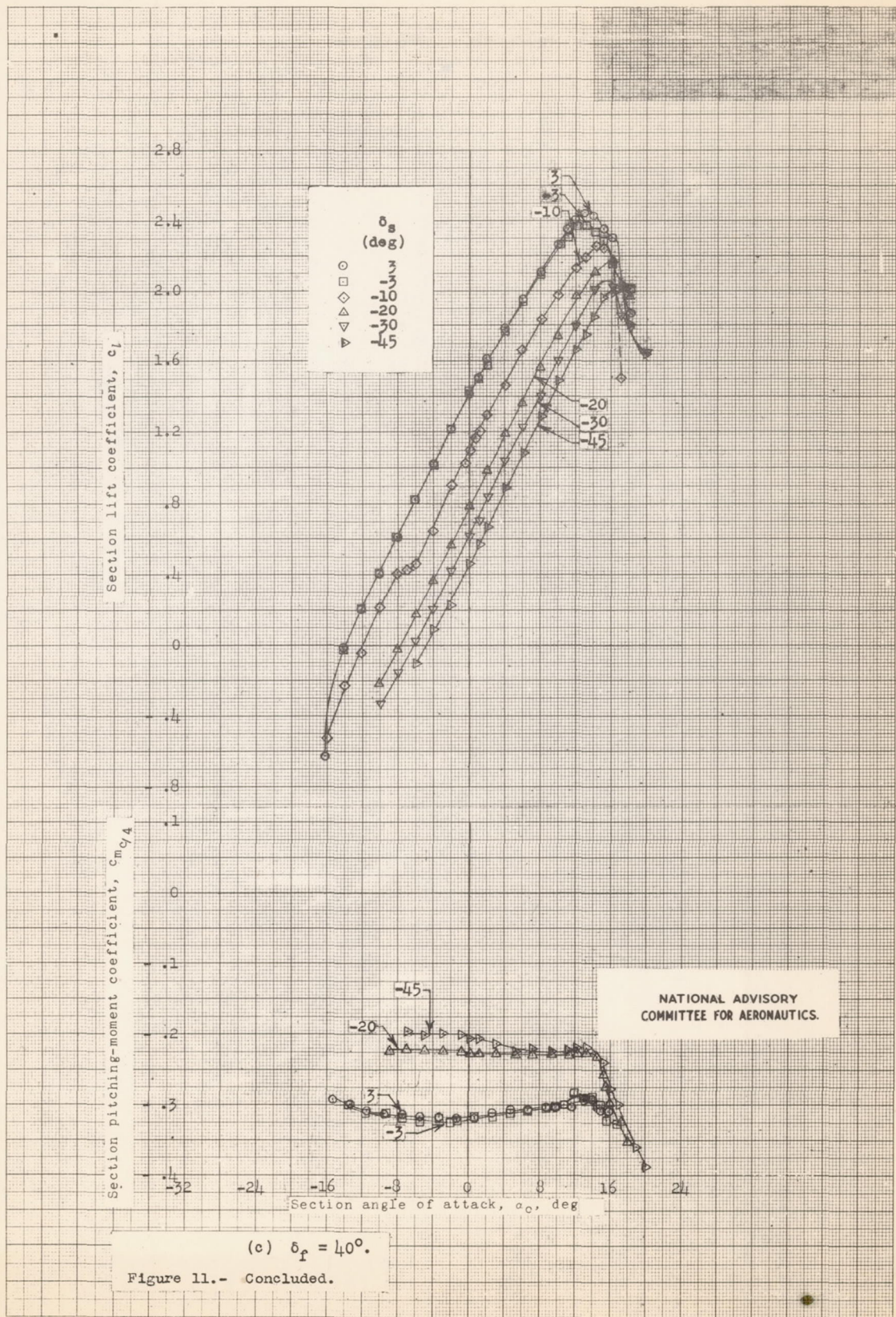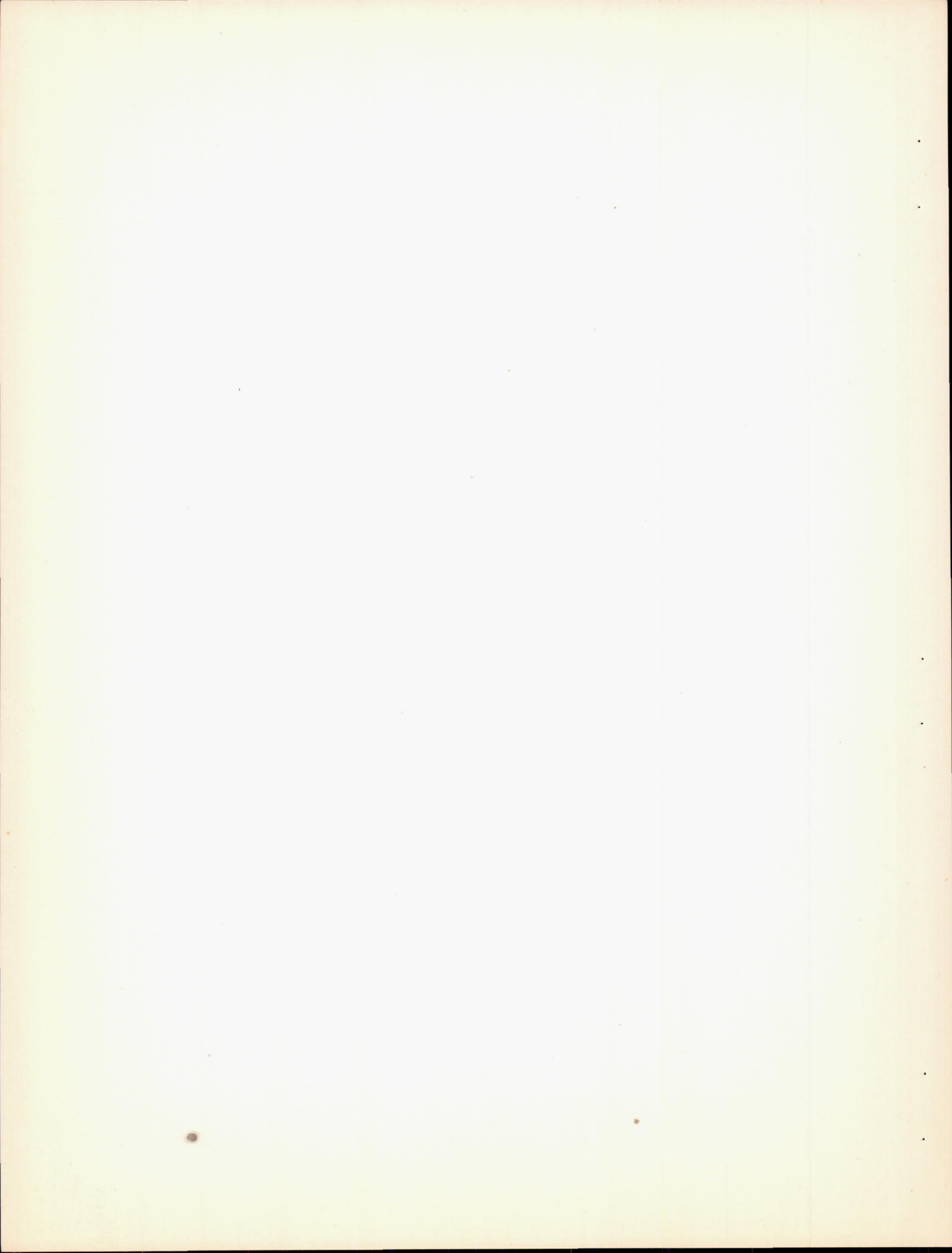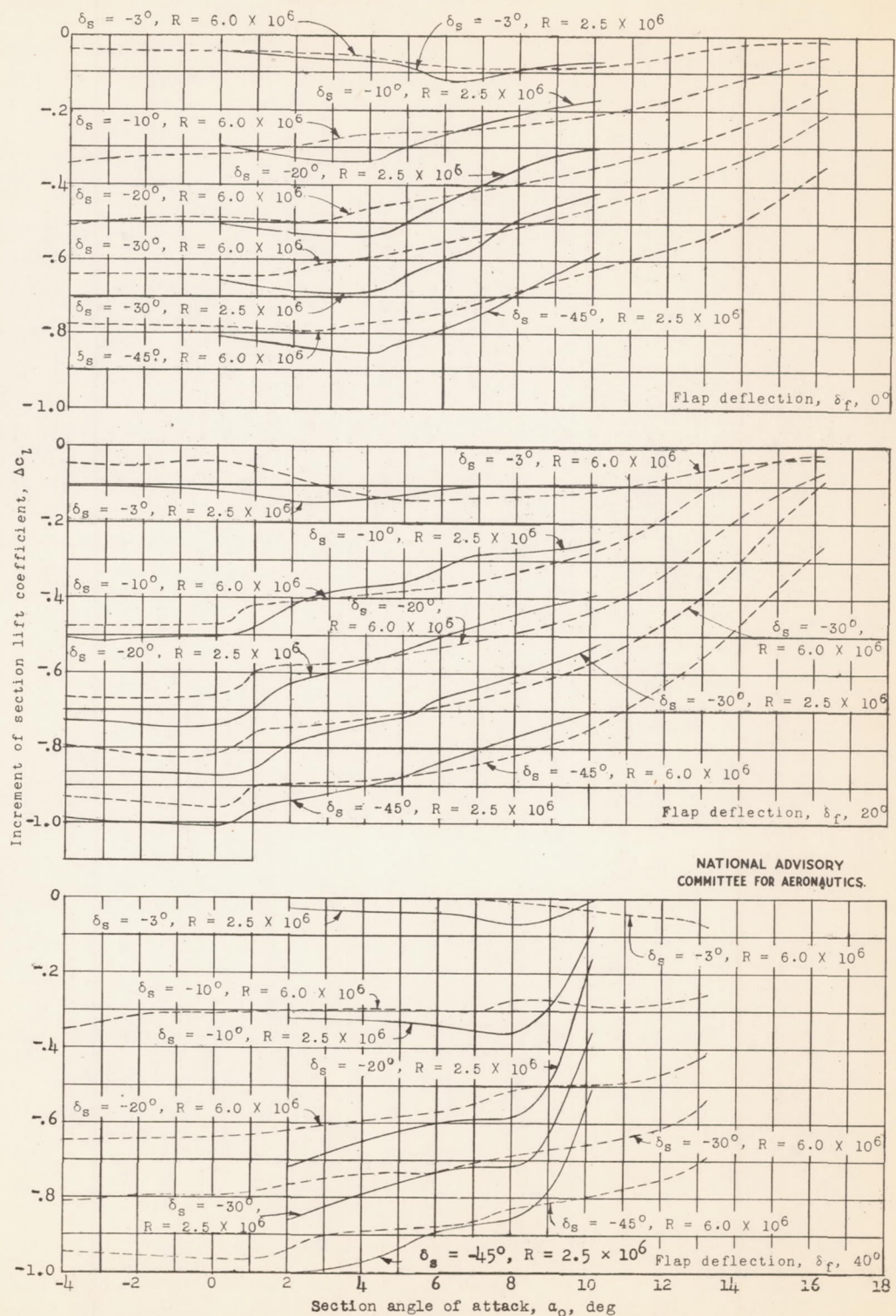
Figure 12.- Variation of the increment of section lift coefficient with section angle of attack for the spoiler flap model for the Hughes XF-11 airplane. Configuration number 9.
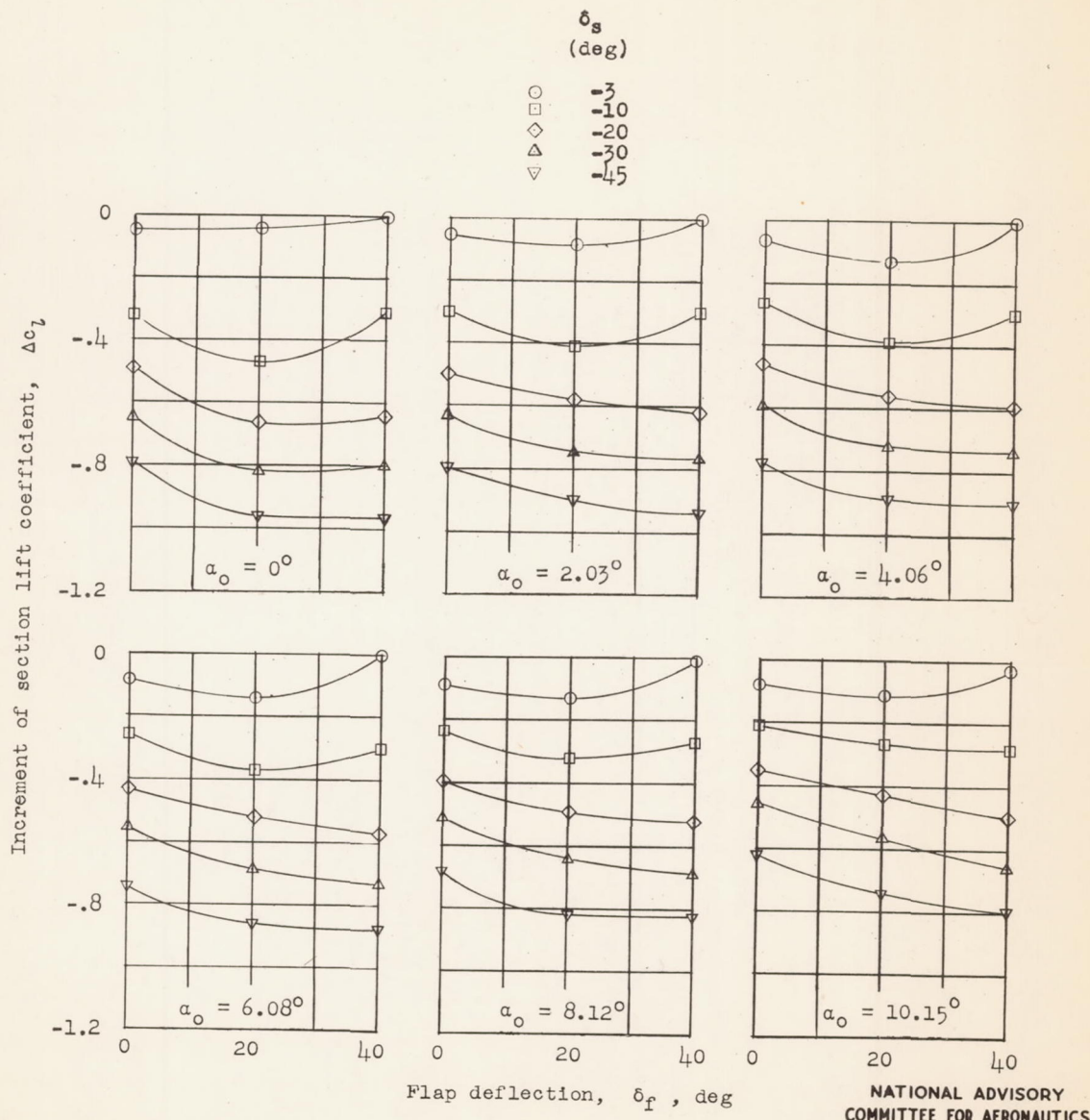
Figure 13.- Variation of the increment of section lift coefficient with flap deflection for the spoiler aileron flap model for the Hughes XF-11 airplane. Configuration number 9; R = 6.0 × 10⁶.
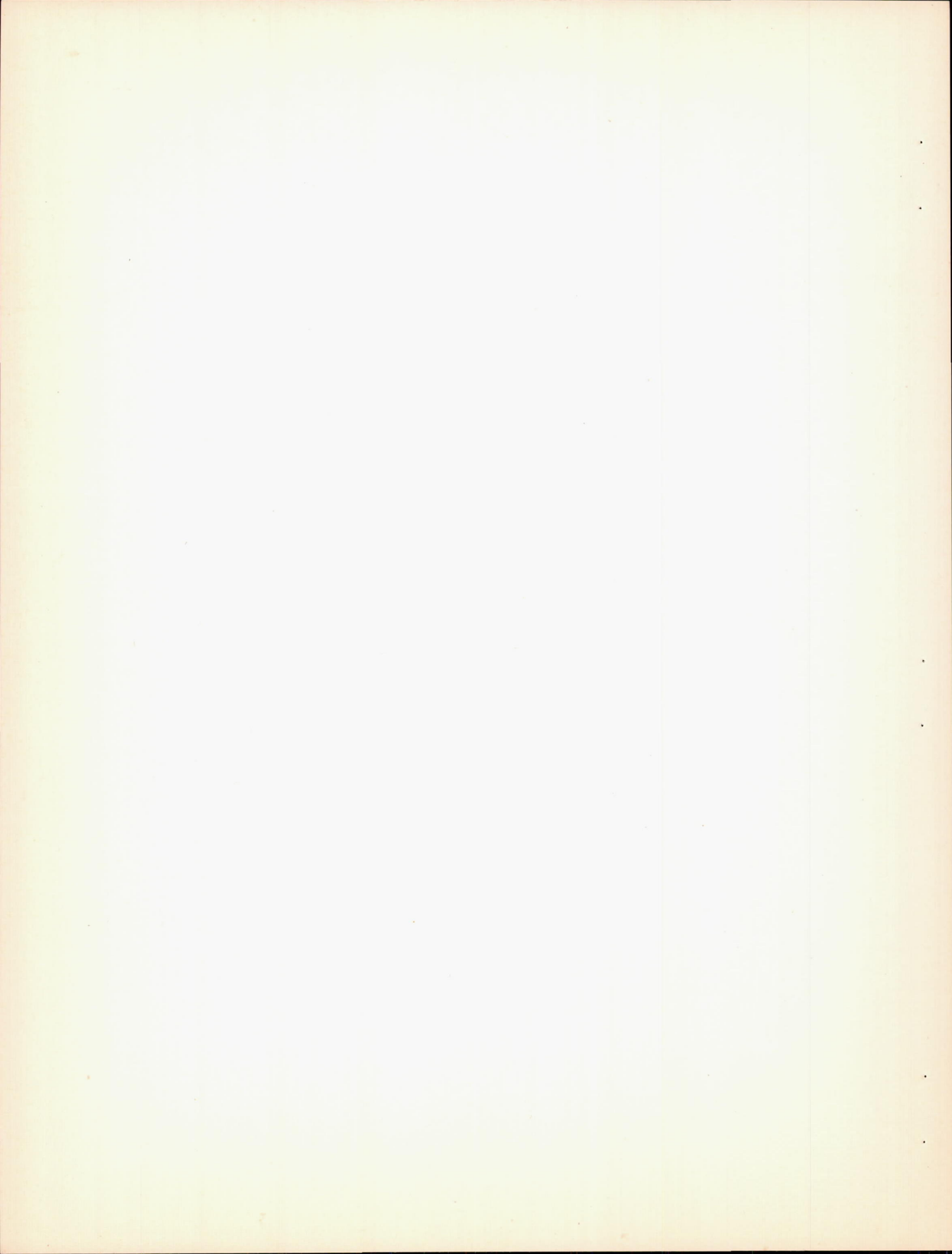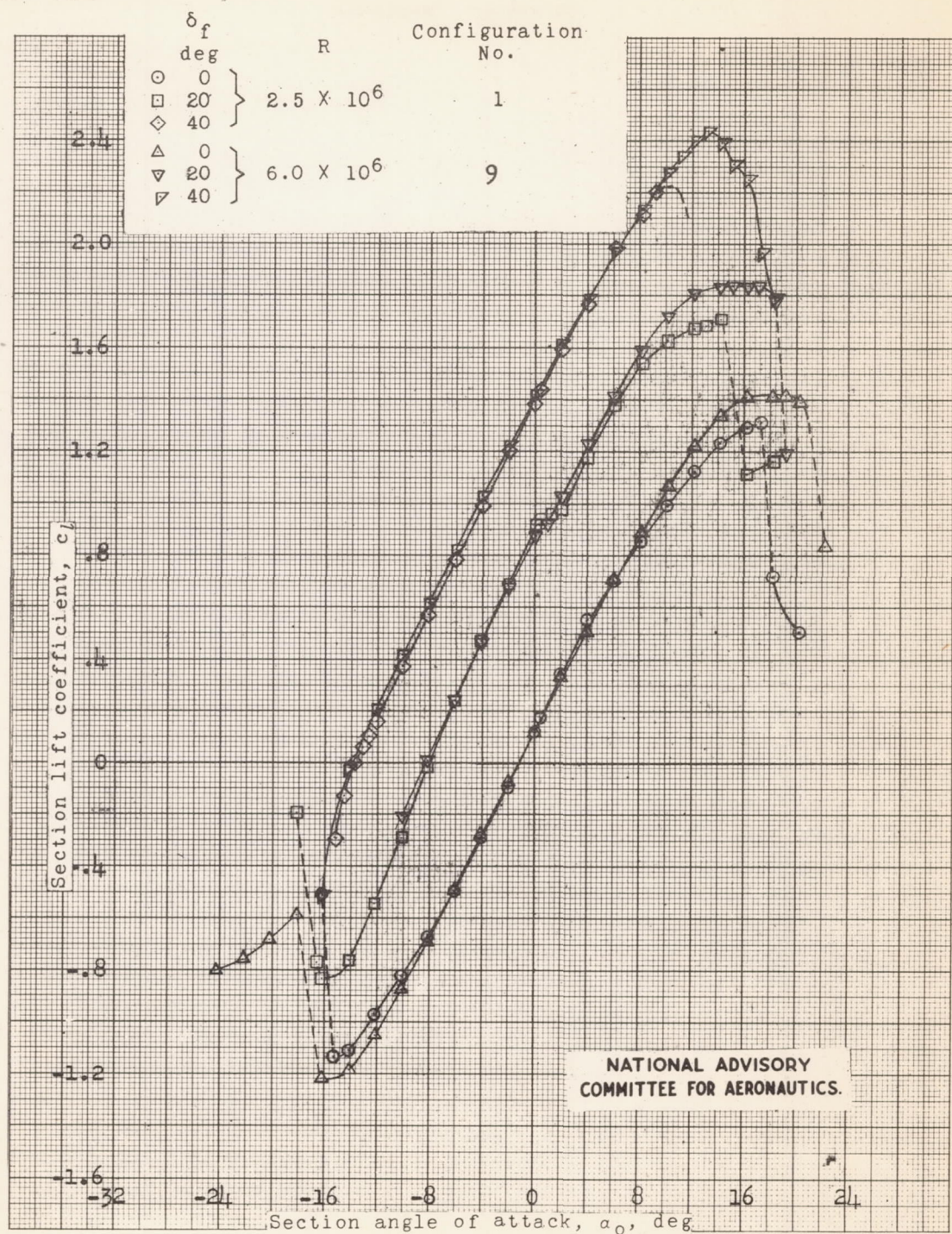
Figure 14.- Variation of section lift coefficient with Reynolds number for flap deflections of $0°$, $20°$, and $40°$. Spoiler aileron flap model for the Hughes XF-11 airplane. $\delta_s = 3°$.

Spoiler deflection

(deg)

▷ -3
◁ -10
▽ -20   R = 2.5X10^6
▽ -30
◸ -45

☉ -3
□ -10
◇ -20   R = 6.0X10^6
△ -30
▽ -45

Flap deflection, δ_f, 40°

Flap deflection, δ_f, 20°

Flap deflection, δ_f, 0°

NATIONAL ADVISORY
COMMITTEE FOR AERONAUTICS.

Spoiler effectiveness parameter, $\dfrac{\Delta \alpha_0}{\Delta \delta_s}$

Section lift coefficient, c_l
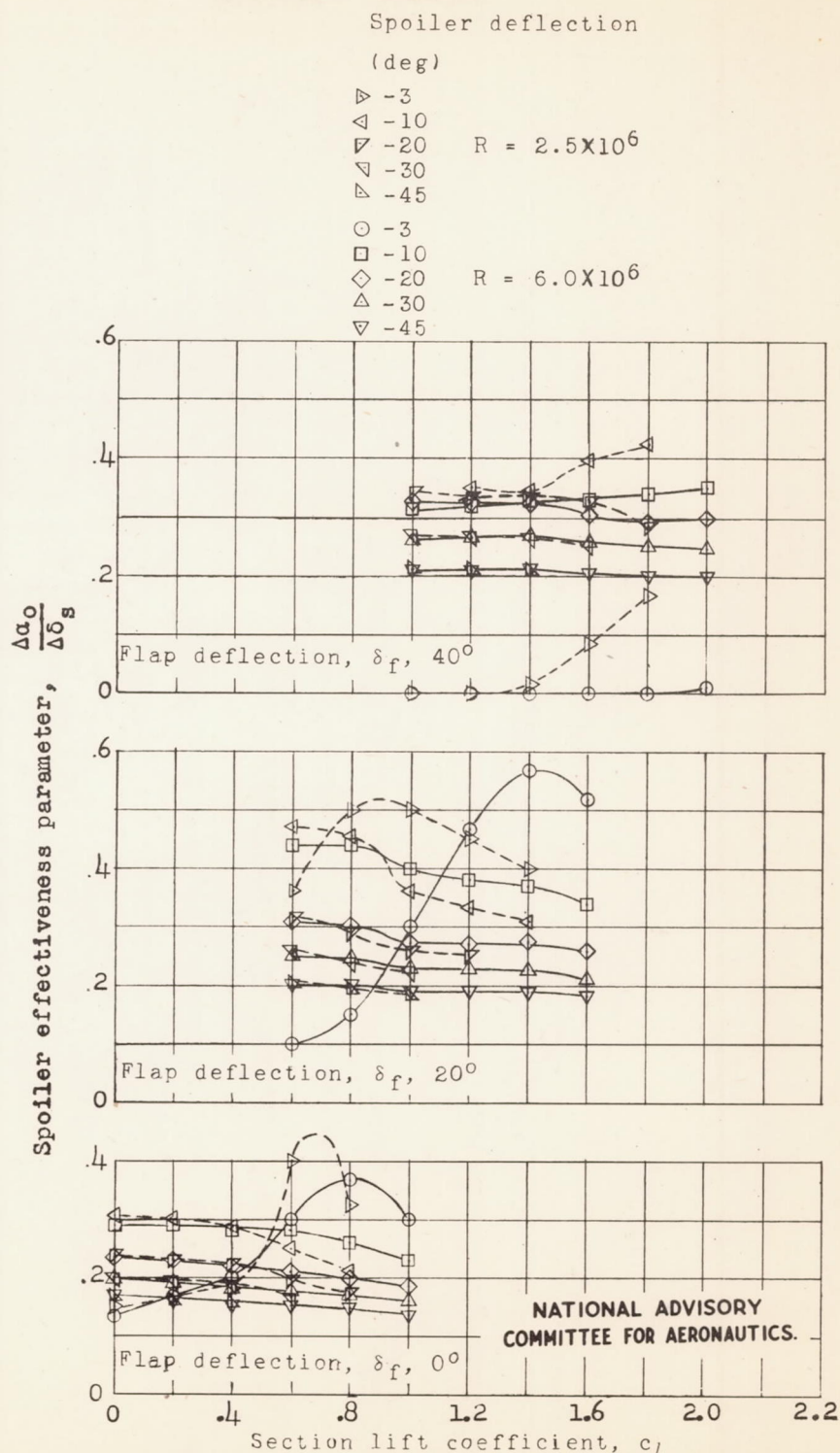
Figure 15.- Variation of spoiler effectiveness parameter, $\dfrac{\Delta \alpha_0}{\Delta \delta_s}$, with section lift coefficient for the spoiler aileron flap model for the Hughes XF-11 airplane.   Configuration number 9.
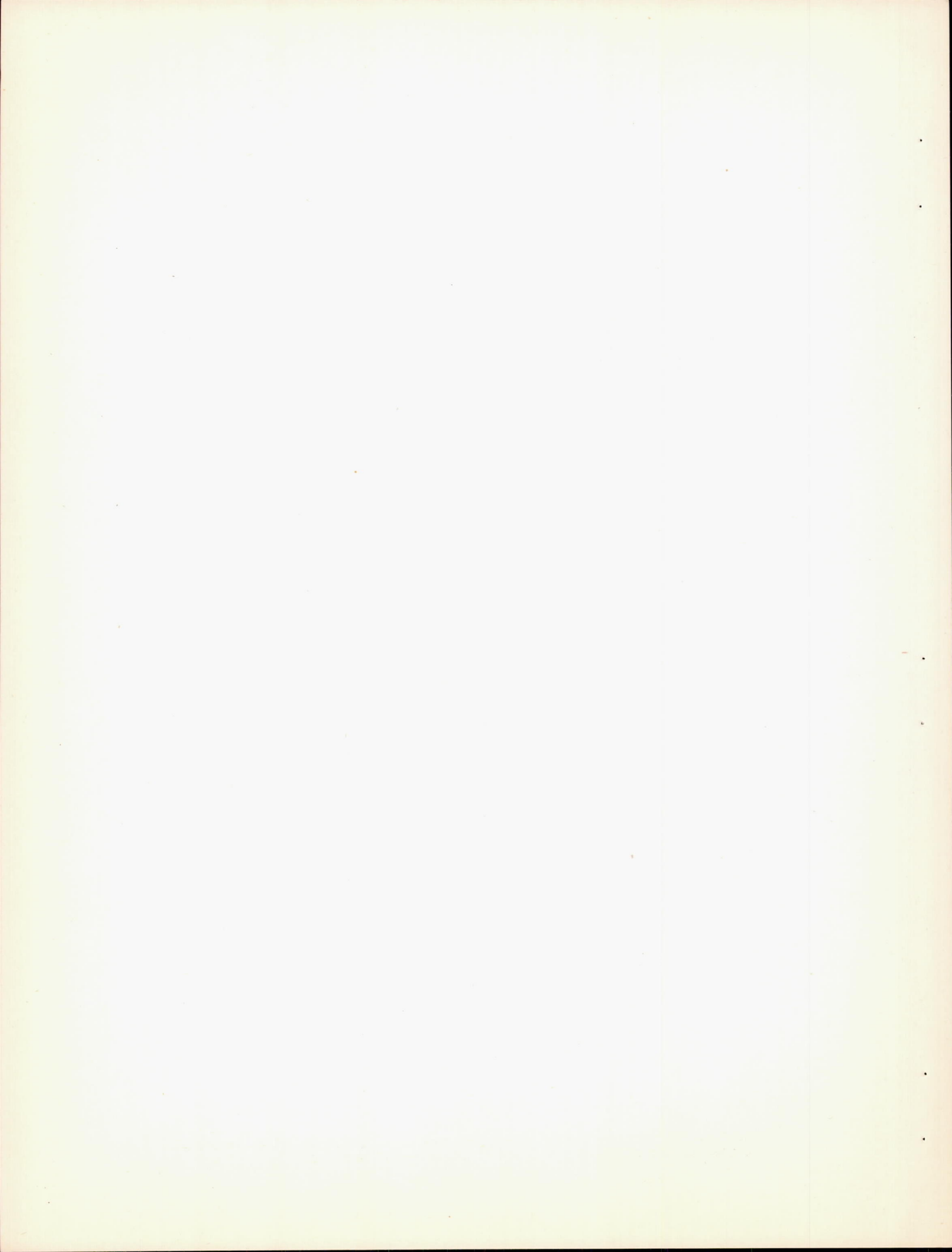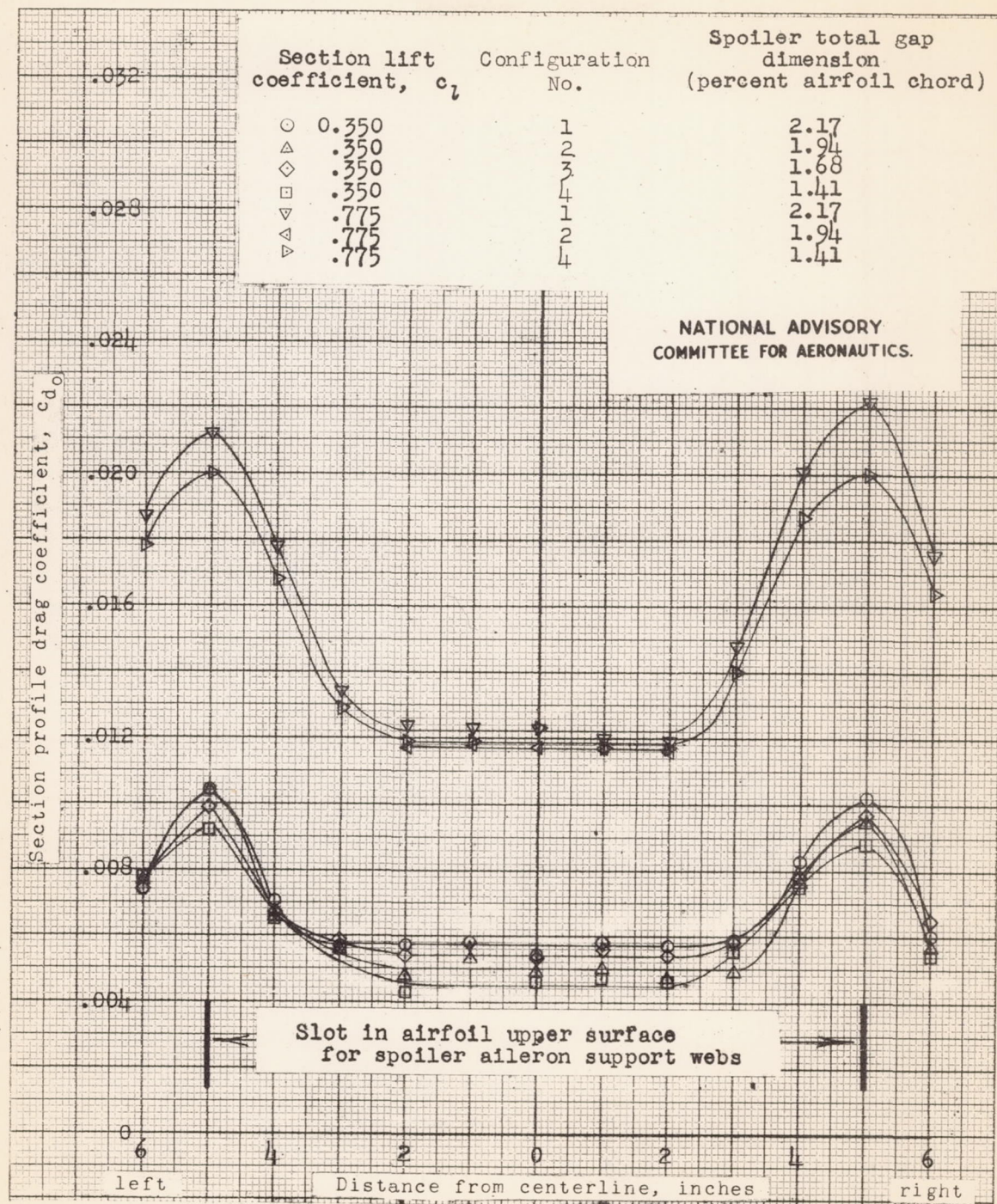
Figure 16.- Spanwise variation of the profile drag coefficient with spoiler rear-gap dimension for the spoiler aileron flap model for the Hughes XF-11 airplane. $\delta_s = \delta_f = 0°$; $R = 2.5 \times 10^6$; LTT test 392.

Section lift coefficient, c_l

○	0.122
□	.331
◇	.503
△	.706
▽	.894
◁	1.223

Section lift coefficient, c_l

□	-0.077
◇	- .281
△	- .488
▽	- .692
▷	- .897
◁	-1.049

Section profile drag coefficient, c_{d_0}

Section profile drag coefficient, c_{d_0}

.032 .028 .024 .020 .016 .012 .008 .004 0

Slot in airfoil upper surface for spoiler web

12 left 8 4 ₵ 4 8 12 right

Distance from centerline, inches

12 left 8 4 ₵ 4 8 12 right

Distance from centerline, inches

Figure 17.- Spanwise variation of the section profile-drag coefficient for the spoiler aileron flap model for the Hughes XF-11 airplane. Configuration number 9; $\delta_s = 3°$; $\delta_f = 0°$; $R = 6.0 \times 10^6$; TDT test 799.
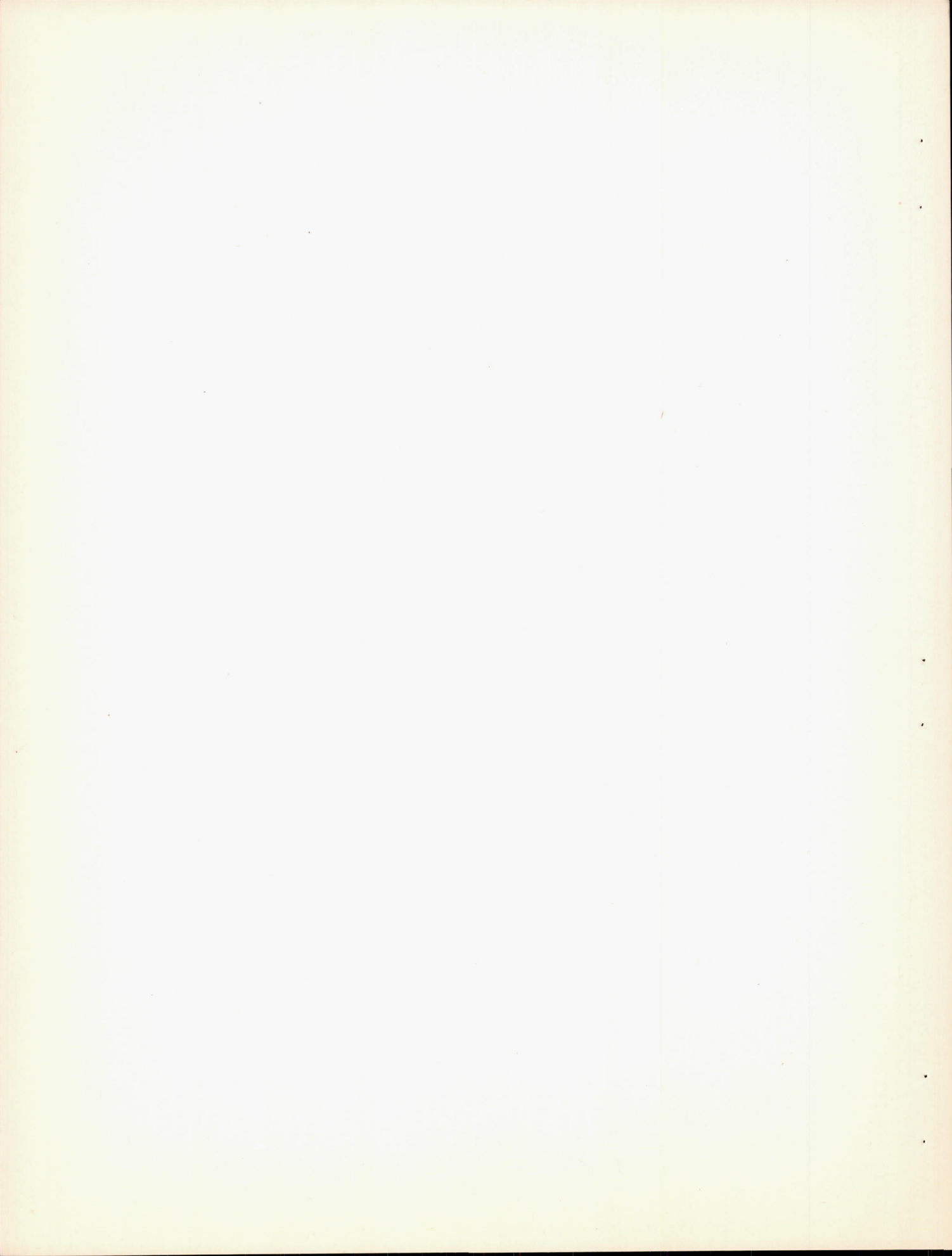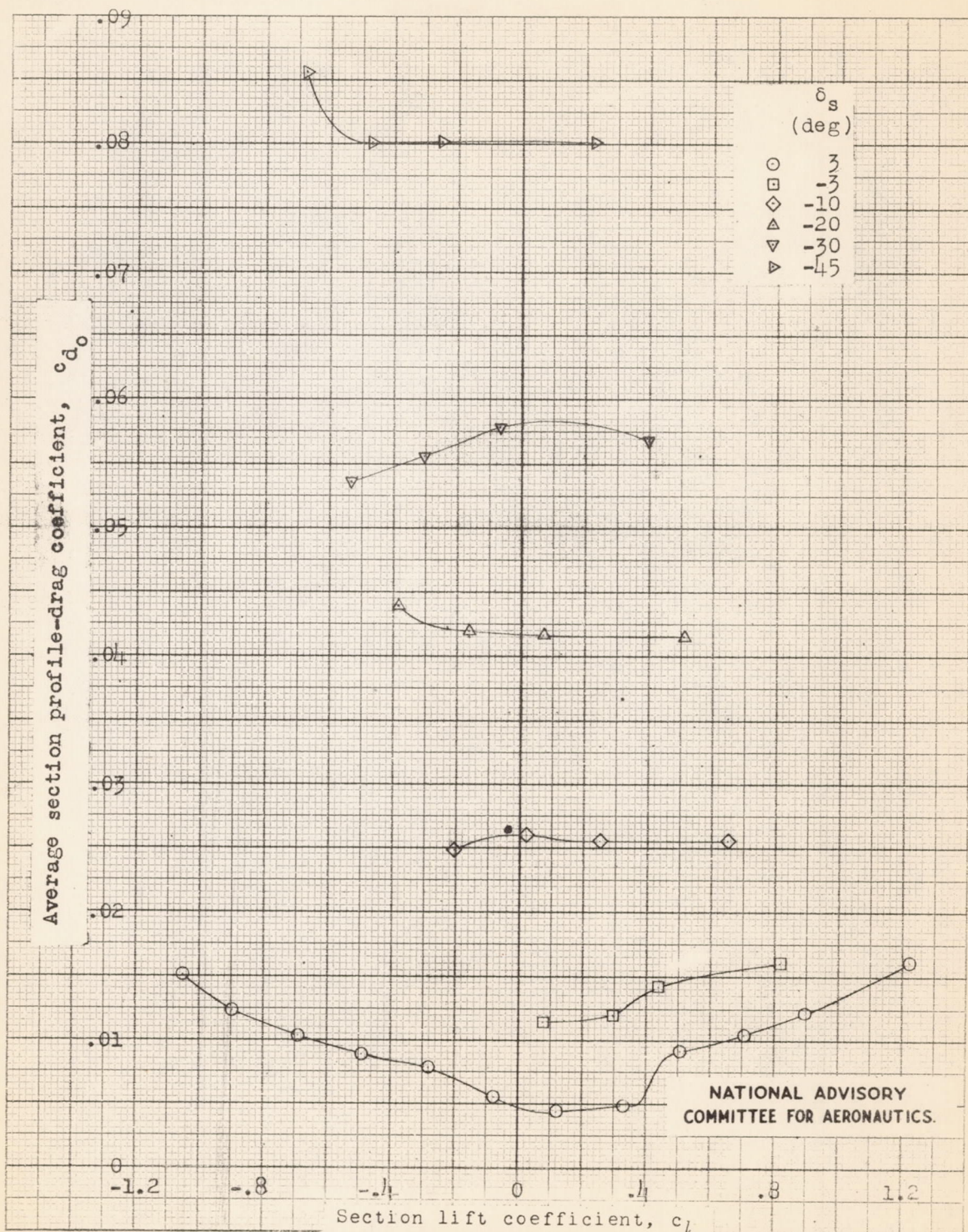
Figure 18.- Average section profile-drag characteristics over a 20-inch-span section of the spoiler aileron flap model for the Hughes XF-11 airplane. Configuration number 9; $\delta_f = 0°$; $R = 6.0 \times 10^6$; TDT test 799.
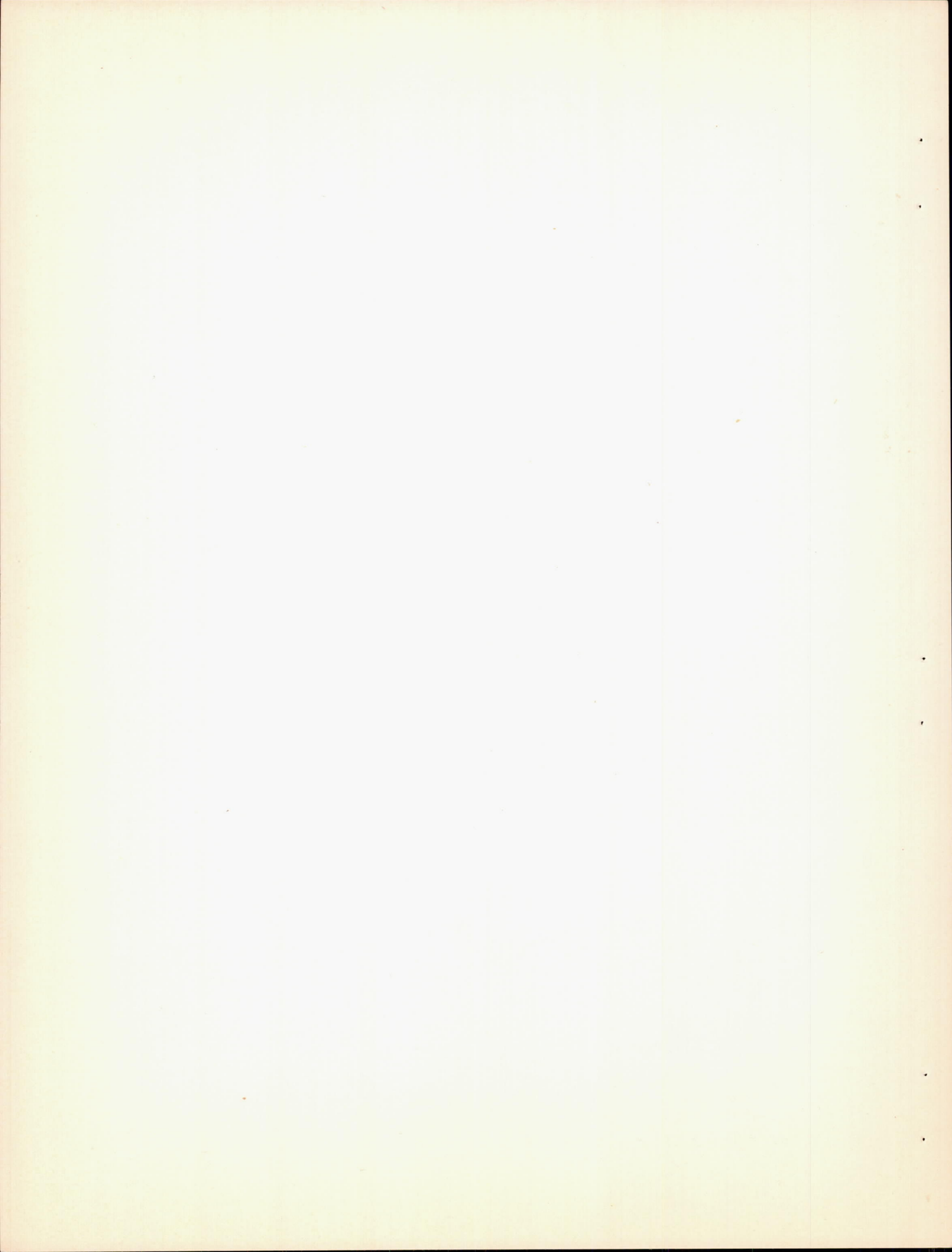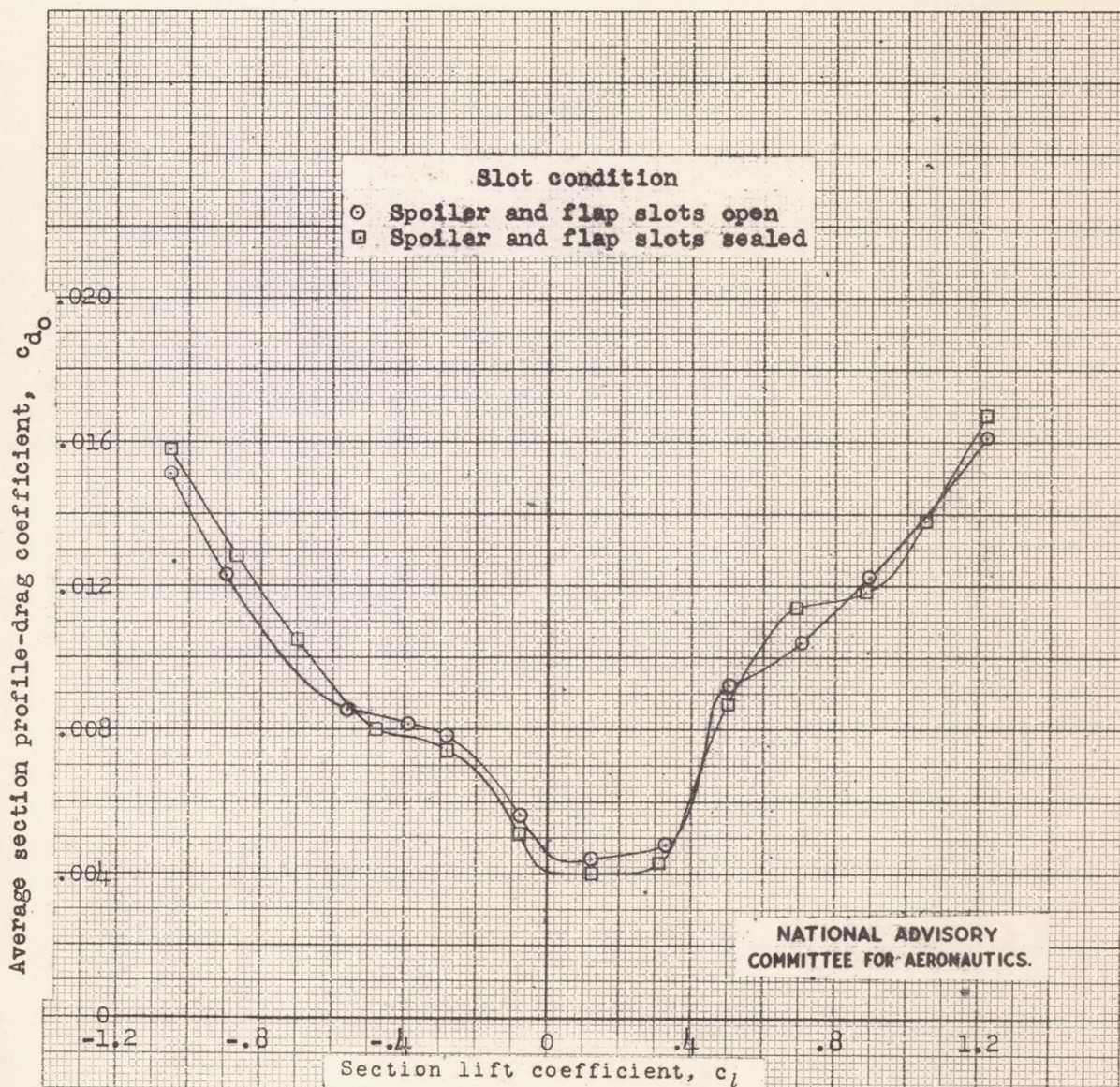
Figure 19.- Average section profile-drag characteristics over a 20-inch-span section of the spoiler aileron flap model for the Hughes XF-11 airplane. $\delta_f = 0°$; $\delta_s = 3°$; $R = 6.0 \times 10^6$; TDT test 799.

NACA 66(215)-216 airfoil with 0.20c sealed plain flap; δ_f , 0° (reference 1)

Increment of section pitching-moment coefficient, $\Delta c_{m_{o/4}}$

δ_f
deg
——— 0
----20
--.40

Section lift coefficient, c_l = 0

δ_f
deg
——— 0
----20
--40

Section lift coefficient, c_l = 0.50

δ_f
(deg)
———0
---20
--40

Section lift coefficient, c_l = 1.00

Increment of section angle of attack, $\Delta\alpha_o$
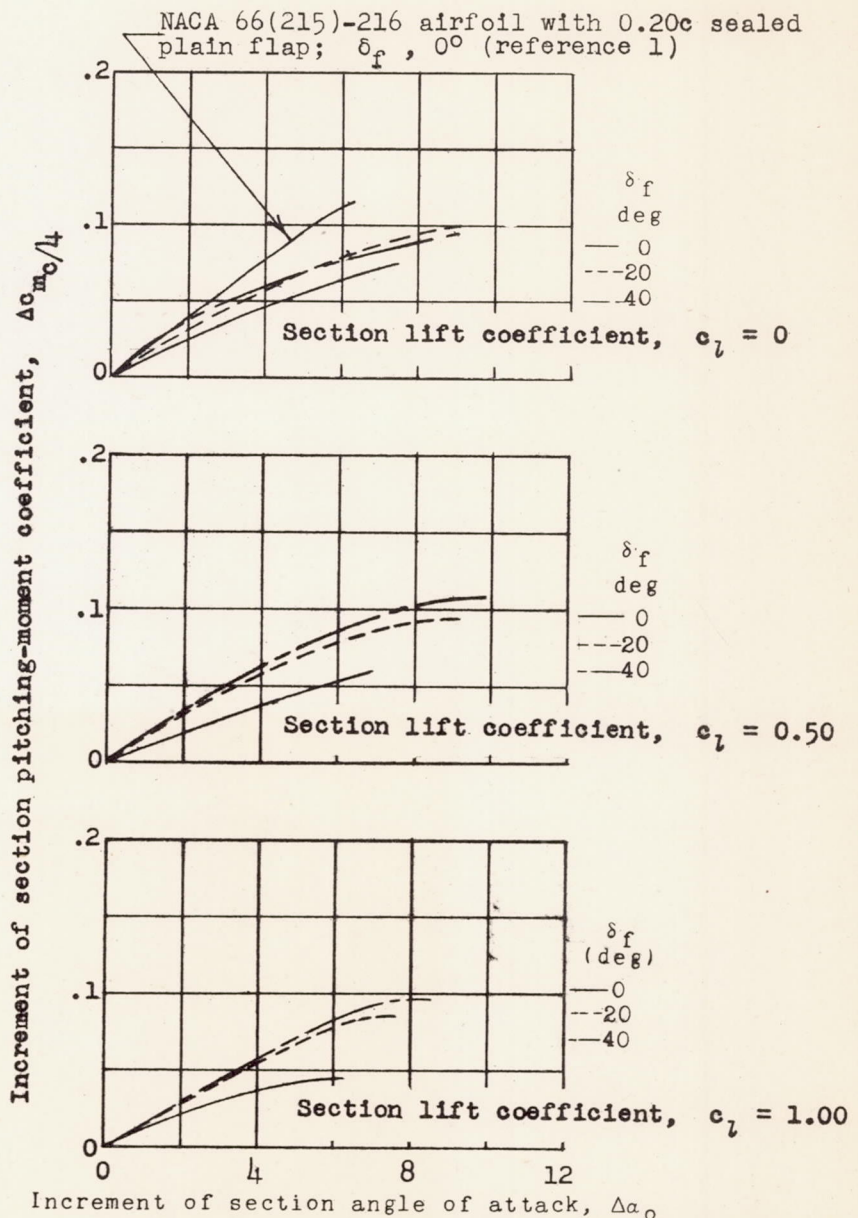
NATIONAL ADVISORY
COMMITTEE FOR AERONAUTICS.

Figure 20.- Variation of the increment of section pitching-moment coefficient with the increment of section angle of attack for the spoiler aileron flap model for the Hughes XF-11 airplane. Configuration number 9.